Published by :
https://www.ijert.org/
An International Peer-Reviewed Journal

International Journal of Engineering Research & Technology (IJERT)
ISSN: 2278-0181
Vol. 14 Issue 12 , December - 2025

Integrated Energy Management and Regenerative Braking Optimization in Fuel-Cell Electric Vehicles Using Multi-Objective Metaheuristics

Adel Elgammal
Professor, Utilities and Sustainable Engineering, The University of Trinidad & Tobago UTT

Abstract: **- This paper proposes an integrated control and optimization scheme for FCEVs, which orchestrates both multi-source energy management (including power generation and propulsion) with regenerative braking to improve efficiency, drivability and components life. The powertrain of the vehicle consists of a proton exchange membrane fuel cell (PEMFC) as prime mover, with battery and supercapacitor to manage peak power requirements and energy recovery. A multi-objective metaheuristic optimizer serves the supervisory layer and determines real-time power-split and braking-force allocation setpoints by minimizing fuel-cell specific hydrogen consumption (SHC), battery aging proxies (RMS/peak current, deep SOC excursions), DC-link voltage deviations, as well as friction-brake usage, while respecting constraints on fuel-cell ramp rate, source current limits, and battery/supercapacitor SOC/voltage windows. Rapid inner-loop controllers are used to control the DC–DC converters and traction inverter d–q currents, ensuring fast time response for DC-link stabilization and torque tracking through maneuvers such as load transients, grade change, or parameter variation. Regenerative braking is co-optimized with energy management, that schedules braking effort between motor regeneration and friction braking, and assures wheel-slip and actuator constraints to get maximum recoverable energy without sacrificing safety. Simulation experiments on standard and aggressive drive cycles, including sweeps in uncertainty (converter L/R drift, DC-link capacitance variation and change in motor parameters) show improved DC-bus regulation, and less torque ripple with robust constraint satisfaction without retuning. Compared to PI-tuned and rule-based baselines, reported results demonstrate that the proposed method achieves up to 13.6%, 10%, and 18.7% reduction in hydrogen consumption, recovered braking energy, and battery stress with better overall powertrain stability. The findings validate that combined optimization of the RBE and multi-objective EM strategy shows practical potential to prolong component life and improve FCEV efficiency in real-world transient driving.**

Keywords: **Fuel-cell electric vehicles (FCEVs), Energy management system (EMS), Regenerative braking optimization, Multi-objective metaheuristics, Battery aging mitigation**

I. INTRODUCTION:

Fuel-cell electric vehicle (FCEV) technology is progressively looked upon as a viable route toward sustainable mobility, since the traction power originates electrochemically by hydrogen through the fuel cell stack and is transferred to the electric drive torque via power electronics and motor drive [1], [3], [6]. A battery (or an auxiliary power unit APU) is typically kept to absorb load transients, capture regenerative braking, and peak-load shave allowing the FC system to be operated from quasi-steady efficient design points both under partial load and under dynamic loads to reduce highly-dynamic operation that would pose additional threats of degradation of the FC system [3], [6]. The hybridization is often pursued further by introducing a supercapacitor/ultracapacitor (SC/UC) in parallel with the battery to make use of its high-power density and fast charge acceptance in situations such as hard acceleration and regenerative braking, which reduces the current spike and enhances the DC-link stability [2], [4], [11]. Some early papers on fuel-cell/battery/SC vehicles have also indicated that attainable fuel-economy and stress-reduction benefits depend highly upon how power is shared, and regeneration is scheduled considering constraint [2], [11]. This results in two closely-interacting layers shaping FCEV performance: The energy management strategy (EMS), distributing traction power between fuel cell, battery and SC on multiple timescales [3], [4], [6].The regenerative braking system (RBS) controlling to what extent regenerative wheel powers is electrically captured vs. dissipated by friction brakes, while ensuring safety & stability, and re.t. driver brake feel[18]–[20]. Recent EMS literature range from heuristic rule-based/Fuzzy logic control methods, optimization-based techniques like ECMS/PMP, DP and MPC with an emphasis on trade-offs among fuel economy, durability and real-time implementation [3], [5], [6]. Simultaneously, RBS studies have indicated that achieving full recuperation is seldom a single objective task since braking should be constrained within tire–road friction limits, ABS/ESC margins, actuator saturations, DC-link voltage constraints and battery/SC charge acceptances – all depend on speed, road conditions and component states [18]–[20].

The main problem incentive for integrated EMS–RBS study is that the key targets and constraints are conflicting, coupled and time variant, therefore optimal or near optimal performance seldom can be attained when energy management separately optimizes with regenerative braking[3],[6],[18]. Regarding EMS side, reducing the consumption of hydrogen and protecting fuel-

International Journal of Engineering Research & Technology (IJERT)
ISSN: 2278-0181
Vol. 14 Issue 12 , December - 2025

cell durability usually leads to a flat current of fuel cell implemented by explicit ramp/slew limits, which would resist challenging the fuel cell with sharp power swings [3], [6], [9]. Nonetheless, regenerating more braking energy usually demands a fast deceleration of transient and short-duration negative power spikes which can disrupt the DC bus, exceed battery charge limits or significantly increase the risk of battery aging if such a condition is regularly applied under high C-rate regime [11], [18], [19]. Going beyond of what an RBS would like, full regeneration likely prefers strong motor braking, however safety-critical restrictions (wheel slip limitations; stability margins; brake blending requirements) will often place some fraction of the braking torque to be frictional-based—specifically on low-μ roads or as extreme decelerations [18]–[20], [22], [23]. In the literature, optimisation and wheel slip-aware braking investigations are united in suggesting that attention to braking allocation on a state-dependent basis relative to stability constraints is necessary instead of solely maximising electrical recovery [22, 23]. These trade-offs also vary with drive aggressivity, grade, traffic and uncertainties: aging-induced resistance increase, fuel cell performance degradation, converter parameter deviation (temperature), making fixed rules or gains brittle and leading to multi-objective and adaptive formulations that explicitly handle conflicting objectives [3], [6], [8], [13].

While the level of development is high, there are a number of practical obstacles as to why full integration of EMS–RBS is still hard and many systems rely on neatly layered heuristics. First, online embedding of durability modeling is still challenging. Fuel-cell degradation is also load cycle, start–stop, humidity/thermal condition, reactant starved and transient operation dependent, and literature highlights that estimating such mechanisms to reliable online penalty terms is not a trivial exercise while stack- and system-specific [27], [28]. Battery aging is also multi-factorial (temperature, SOC window, C-rate, depth of discharge, calendar aging), and thus many EMS designs rely on tractable proxies like RMS current, peak current counts and SOC deviation penalties rather than physics-complete electrochemical aging models [11], [13]. While proxies are useful, their estimates may differ from the real lifetime results—especially considering uncertainty and temperature fluctuation [11], [13]. Second, the coupled problem is multi-time-scale and tightly-constrained. Inner current/voltage loops, inverter control represent events (co:2∗10 3 ms) braking actions can switch within tens of milliseconds, whereas higher level supervisory functions for power management are updated at 100−ms based on the performance constraints [3],[10], [18]. MPC-based frameworks are appealing as they implicitly encode predictions and hard constraints, yet the complexity increases with model accuracy, horizon length, non-convex efficiency maps, and switching logic being counter-productive for time deployment without significant simplification [3], [10]. These issues are exacerbated when two mainpack energy sources (EMS, RBS) are further co-optimized as both the forward and reverse active power (traction/regeneration) have to simultaneously meet voltage/current/SOC/voltage/braking stability constraints [18]–[19], [22]. Thirdly, it is inevitable that driving and braking are uncertain and non-stationary, parameter drift. EMS benchmarks and AI-biased surveys agree on the fact that cycle adaptability can be enhanced by learning-based methods such as DRL, but safety certification, constraint compliance and generalization when going to production are challenges for automotive deployment [14]–[16]. Furthermore, real-world uncertainty (converter L/R drift, DC-link capacitance variation, motor Rs/L changes, battery ESR rise) can potentially erode stability margins for fixed-gain controllers and effectively override threshold-based logic, leading to possible excursions of the DC link, overuse of the batteries (or exceeding safe slew rates/accelerations in fuel cells) [3], [6], [8]. Dispatching and Control This includes policies such as minimization of specific modes of emissions, or maximization of energy efficiency; it also includes methods to build predictive control sequences (e.g., with DP) that are not in real-time actionable for embedded deployment, leading to close-to-real-time solutions that impose the approximation prone ECMS or PMP strategies (fast but tuning-sensitive), or hierarchies combining a slower supervisory optimization approach and robust fast inner loops [7]–[10]. For this reason, the field is still looking for approaches that: (i) address multiple conflicting objectives; (ii) enforce hard constraints; and (iii) are computationally tractable in real-time without frequent retuning under diverse operating scenarios [3], [6], [18].

Control rule-based (CRB) and CRB mixed with fuzzy-logic approaches continue to be popular in FCEVs, as they can provide interpretability, are easy to compute and can impose the intuitive “role separation” (FC supplies average/low-frequency power; battery supplies midfrequency deficits; SC provides fast transients) [3], [4], [12]. Such a structure is in keeping with each source's physical super strongness and lifetime-aware hybrid storage policies [11]. Nonetheless, large-scale reviews also attempt to focus on the limitations of heuristic techniques which can lead to excessive battery cycling, violation of fuel-cell ramp down constraints or even generation of DC-link excursions if operation is dissimilar to the one applied during tuning/calibration [3], [5], [6]. Optimization-oriented EMS The shortcomings in a heuristic-based operation can be addressed more systematically by an optimization-based methodologies of EMS. ECMS maps applied electricity consumption into an equivalent hydrogen consumption and can be calculated in real time; studies on fuel-cell/battery/SC topologies indicate enhanced hydrogen economy, as well as reduced fuel-cell current ripple when equivalence factors are properly adjusted [7]. Adaptive ECMS generalizes the idea of dynamic programming inherent in series HEV supervisory control as it updates equivalence factors and specially accounts for aging subsequently enhancing the robustness to varying operating conditions and degradation due to aging [8]. Real-time energy management with a PMP approach furnishes a theoretical structure for trade-offs between fuel economy and durability-based penalties, which has already been illustrated for fuel-cell hybrids under realistic restrictions [9]. MPC provides predictive constraint handling and it has been used for fuel-cell–battery–supercapacitor systems (e.g., transit applications), although the real-time implementation is still relying on simplified models and an elaborate computational design [10]. DRL has been recently tested in the energy management of FCEV charging to further increase the flexibility and leverage driving data, however a number of prior works warn that constraint satisfaction and verification are still serious bottleneck for safety critical deployment [14]–[16]. In the braking domain, expert RBS studies indicate that there is a need for maximum energy recovery to coexist with braking safety and

International Journal of Engineering Research & Technology (IJERT)
ISSN: 2278-0181
Vol. 14 Issue 12 , December - 2025

stability, resulting in blended brake designs whereby motor regeneration and friction braking are integrated under ABS/ESC and tire–road conditions [18]–[20]. It has been investigated in the context of energy recovery versus stability balance within an optimization-based braking distribution [22], and wheel-slip-aware regenerative braking has been discussed explicitly for in-wheel or electrified drivetrains. Integrated RBS–ABS studies indicate that RB must be actively coordinated with slip control, especially on road surface with changed friction [23]. Together, these studies demonstrate that braking recovery can no longer be assumed to be a "bonus" tacked on after EMS optimization; instead, it must be co-optimized with electrical limits (DC-link over-voltage risk, converter limits) and charge acceptance for storage—especially during aggressive regeneration peaks [18], [19], [22].

To fulfil those lines, this paper develops an integrated EMS–RBS scheme with traction power split and regenerative braking assignment aggregated into a common multi-objective constraint optimization problem to manage by a metaheuristic (multi-objective) at supervisory level under consideration fast inner loops (DC–DC regulation, inverter d–q current control, fuzzy/robust compensation) for high bandwidth dynamics [10], [12], [18]. One pivotal insight derived from the literature is that hierarchical control mimics the multi-time-scale of FCEVs; strong inner loops guarantee fast DC-link stabilization and torque tracking while a slower optimizer updates setpoints to keep multicriteria optimality as operating conditions change [3], [10], [18]. Multi-objective metaheuristics, for instance NSGA-II and MOPSO, are good candidate to solve it due to these methods can handle approximately Pareto-optimal trade-offs under nonconvex problems with mixed constraints, efficiency maps and switching behaviors without the explicit gradients [24]–[26]. NSGA-II [25] offers a common choice of Pareto front construction with diversity preservation, and MOPSO [24], [26] provides a swarm approach based on the repository that is able to achieve a fast convergence due to which it can be combined with warm start and constraint filtering for online or receding-horizon supervisory updates. Based on these and similar integrated EMS–braking studies reported for FCEVs [17], the key elements of the present contribution are: (i) an explicit, simultaneous optimization of hydrogen consumption, DC link regulation, battery stress "proxies", and friction-brake use—the pareto-improvement map spanned by a range of operating regimes is emphasized; (ii) constraint-aware setpoint generation respecting fuel-cell ramp/slew limits and storage/device bounds; (iii) practical real-time division-of-labor in which the optimizer runs at a slower rate than its inner loops but warm starts preserve speed/convergence benefits.

II. Powertrain and braking system architecture for the proposed integrated energy management and regenerative braking optimization in a fuel-cell electric vehicle (FCEV).

The holistic FCEV powertrain and braking system is presented in Fig. 1, which allows for the simultaneous optimization of traction power split control and regenerative braking recovery. On the main power line, the fuel-cell stack produces DC power is fed to a common DC-link by means of an unidirectional DC/DC converter controllable so as to adjust operating current of said fuel-cell and stabilize voltage handling said bus according to constraints imposed on said fuel- cell such as maximum ramping rate and optimal operation point far away from low-efficiency zones. The battery and the supercapacitor are connected to a common DC-link via two bi-directional DC/DC interfaces such that both devices can either supply power for traction demand or sink power during regeneration. This shared DC-link architecture is minatory for coordinated energy management as it allows instantaneously re-allocation of power between the sources and sinks while keeping the uninterrupted drivetrain operation.

When in traction the DC/AC invertor produces 3-time phase power from the DC-link power to drive the electric machine. The motor torque is determined by the driver power request and vehicle dynamics, and the energy management layer distributes the necessary electric power among fuel cell stack, battery pack, and supercapacitor. The role of the fuel cell in normal operation will be to supply the average or "base-load" power because it has a high specific energy and efficiency at steady state, with the battery handling fluctuations above and below some mid-level frequency, while keeping SOC within its targeted window. The supercapacitor, with its high power density and quick charge–discharge characteristics, is intended for high frequency transients (e.g., rapid acceleration events, launches and sudden grade changes). This device division of labor reduces stress on the fuel cell (by constraining fast current swings), mitigates battery peak currents (and aging concerns thereof) and assists in DC-link voltage regulation under aggressive driving conditions.

The regenerative braking path and the braking constraints that dictate energy regeneration is illustrated in bottom part of Fig. 1. As the vehicle driver demands deceleration, the traction motor is ordered into gen mode and inverter negates torque to convert kinetic energy of vehicle into electrical power on DC-link. This restored power is selectively directed to the energy storage devices based on in the respective instantaneous charge acceptance of the energy storage devices. Typically, priority is given to the supercapacitor as it can accept high regenerative peaks with low voltage sag and conversion losses, capturing braking power that may be dissipated as a result of charging current limitations. The battery subsequently captures the remaining regenerative energy complying with SOC constraints, maximum charge current and thermal limitations. If neither's state of charge is available to accept the requisite regeneration power – for example, if in high SOC, at low temperatures or when the requested braking torque exceeds that which can be supplied by machines [d] history mechanical friction brakes provide the remainder.

International Journal of Engineering Research & Technology (IJERT)
ISSN: 2278-0181
Vol. 14 Issue 12 , December - 2025

In Figure 1, the "braking constraints" block describes the physical and safety limitation set which constrains a realistic brake blend strategy. The total drive force (or moment) required at the wheels is limited to what can be provided by tire/road adhesion and vehicle stability, being therefore also limited by the maximum deceleration that can be achieved without wheel spin. Inside that envelope, regenerative braking is also capped by the motor/inverter maximum negative torque and the DC-link voltage constraints jointed with storage-side charge acceptance (battery C-rate, supercapacitor voltage top, and converter current limits). Accordingly, control strategy is not just about maximizing regenerative power all the time, but maximizing recoverable energy without: (i) failing to deliver demanded deceleration, (ii) using friction braking unnecessarily, (iii) compromising component limits, and (iv) disrupting transition of torque among various sources as smooth transitions are desired in order to maintain driveability and avoid brake feel. The explicit representation of their traction and regeneration behavior in a unified architecture reflects the couples nature of the problem: decisions that maintain SOC headroom for batteries and voltage margin for supercapacitors during traction operation immediately pay dividends on the ability to recapture regenerative braking power.

Figure 1 justifies the use of multi-objective metaheuristics even further by showing how conflicting goals emerge from these interactions. Over-utilizing the battery as a traction control can cause short-term consumption of fewer hydrogens and but push up SOC or excite higher temperature, lower the capacity of regeneration or promote decline. Conversely, with a mid-range SOC and super capacitor headroom reserved for increased regenerative capture and transient response, but potentially more difficult in terms of the fuel cell to contribute higher average power and hydrogen usage and fuel-cell dynamic stress. Hence, the architecture offers a unifying optimization of power-split and brake blending optimizing hydrogen economy, energy recovery DC-link stability and component health in coordination satisfying the traction and regenerative limits as illustrated also in in Figure.

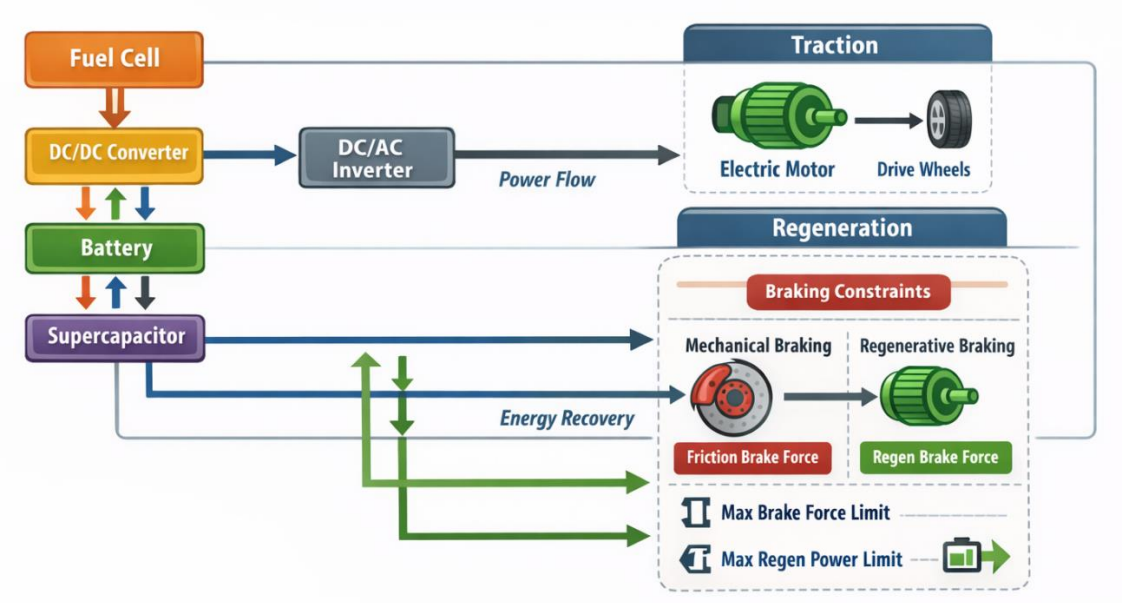

Figure 1. Powertrain and braking system architecture for the proposed integrated energy management and regenerative braking optimization in a fuel-cell electric vehicle (FCEV). The fuel-cell stack supplies the DC bus through a DC/DC converter, while the battery and supercapacitor exchange bidirectional power to support load transients and maintain DC-link stability. A DC/AC inverter drives the traction motor for propulsion, and during deceleration the motor operates as a generator to recover braking energy. Regenerative braking is coordinated with mechanical (friction) braking under key constraints, including total brake force demand, maximum allowable regenerative braking force/power, and component charge–discharge limits, ensuring safe braking performance while maximizing energy recovery.

The end-to-end process to achieve integrated energy management and regenerative breaking optimization in a fuel-cell electric vehicle (FCEV) was demonstrated in Fig. 2, highlighting the transfer between an offline multi-objective design phase and a real-time, constraint-aware control implementation. This starts in the inputs block where typical driver pattern (urban-highway mix, stop-go intensity, grade profiles, and transient events) are coupled with a validated vehicle longitudinal model together with detailed models for fuel cell/battery/supercapacitor as well as its associated DC - coupling converters and the appropriate DC - AC inverter/motor dynamics. Importantly, the input layer also handles braking constraints that characterize both safety and feasibility during deceleration operation (e.g., maximum allowable total brake force, and motor/inverter regenerative torque limits, DC-link voltage bounds, battery charge current/SOC ceilings, supercapacitor voltage limits). As the braking constraints are imposed at the input so much, the figure really captures what is - in fact - one of the core messages of the paper: regenative capability is not just an

International Journal of Engineering Research & Technology (IJERT)
ISSN: 2278-0181
Vol. 14 Issue 12 , December - 2025

ancient history thought added to (separately represented from) a propulsion system model and its limits must be considered together with those associated with traction power allocation and storage state management.

The central part of Figure 2 refers to the off line optimization phase, in which a multiobjective metaheuristic (e.g., NGA-II, MOPSO or variants) inspects a large decision space for computing not only one operating point but a set of Pareto-front solutions. In this step, candidate control strategies (commonly parameterized rule- or schedule-based or weighting-factor-based or policy-map-based) are assessed over the drive-cycle set to assess trade-offs between competing objectives such as hydrogen/fuel economy, regenerative energy recovery, and compromise on component stress and degradation proxies (fuelcell current ripple/ramp penalties, battery RMS/peak current and supercapacitor cycling), with drivability assessments for torque smoothness, brake-blending continuity as well as avoidance of oscillatory power sharing. As the objectives are inherently conflicting (e.g., minimizing H2 may lead to load battery, maximizing regeneration would imply to keep some SOC/voltage headroom), the optimizer returns a set of trade-off policies. This Pareto set is then used as a "benchmark library" that characterizes the trade-offs to be expected when trading off different preferences and operating regimes, whilst keeping all the solutions feasible (in terms of physical constrains) from powertrain and braking systems.

Figure 2 The deployment process of these offline obtained results in the online control operation is shown on the right side of Figure 2. To this end, real time data on the driver traction/brake request (or demanded wheel torque), vehicle speed, DC-link voltage, battery SOC/temperature/charge acceptance and supercapacitor voltage are provided to a supervisory layer that performs optimal policy lookup and on-line updating. Concretely, this is realised by following the Pareto-optimal policy (or interpolating between them) that fits the current circumstances and priorities best, before slightly modifying setpoints to compensate for disturbances and model mismatch. Output of this online decision stage is a coordinated set of powertrain and braking commands which execute, two closely inter-related actions: (i) power management during traction operation(Power split control), determining what part comes from the fuel cell and how much is supplied by buffer devices i.e., battery and supercapacitor-; and (ii) regenerative braking control during vehicle deceleration(brake blending), determining how much regen torque can be provided by motor, while still requiring some friction brake to ensure a safe meeting of total demanded decceleration.

The feedback arrows in figure 2, although not bi-directional, show this is not an open-loop strategy. At each time instant the controller uses actual DC-link voltage, realized wheel torque produced, fuel-cell response and state of charge trajectories to improve the following step decisions and constraints. This feedback is of particular importance at transitions from traction to braking or on rapid changes in deceleration demand when regeneration can be suddenly restricted by motor speed, inverter current limits, or storage charge acceptance. By combining offline Pareto-based policy generation and online selection-and-adjustment, the provided framework in Figure 2 shows how it can simultaneously (i) maintain drivability and brake safety, (ii) protect operates from maximum stresses, and (iii) optimize energy capture/reuse while minimizing hydrogen consumption over realistic driving profiles.

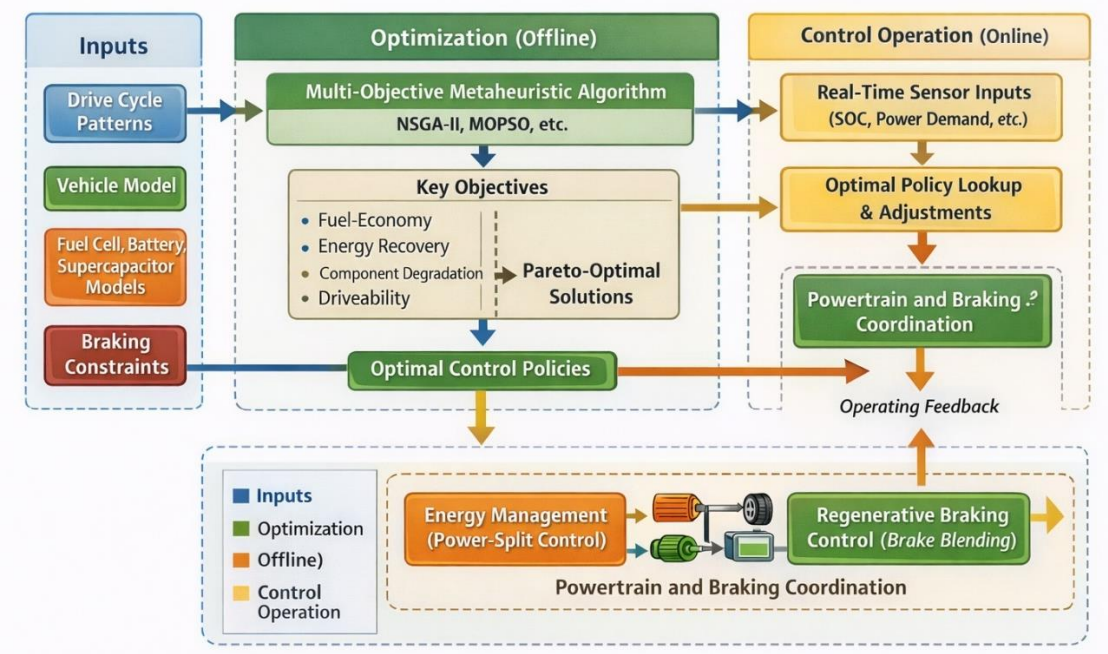

Figure 2. Workflow and control operation of the proposed integrated energy management and regenerative braking optimization framework for FCEVs. Offline, representative drive-cycle patterns, validated powertrain component models (fuel cell–battery–supercapacitor with converter/inverter dynamics), and braking constraints are supplied to a multi-objective

International Journal of Engineering Research & Technology (IJERT)
ISSN: 2278-0181
Vol. 14 Issue 12 , December - 2025

metaheuristic optimizer (e.g., NSGA-II, MOPSO) to generate Pareto-optimal control policies that balance hydrogen consumption, regenerative energy recovery, component stress/degradation, and drivability. Online, real-time measurements (power demand, vehicle speed, SOC/voltage limits, and braking request) are used to select and adapt an appropriate policy, which then coordinates (i) power-split commands among the fuel cell, battery, and supercapacitor and (ii) brake blending between regenerative and friction braking. Operating feedback is returned to update decisions and enforce constraints continuously over the drive cycle.

III. Simulation Results and Discussion

To validate the proposed integrated energy management and regenerative braking optimization scheme (Figures 1–2), a high-fidelity power-split Ref FCEV model was developed within a backward/forward hybrid simulation environment (such as MATLAB/Simulink-style architecture). The powertrain then tracks the driver speed trace with a PI speed controller which yields the requested wheel torque. This torque request is then transformed into an electrical traction power command using the motor–inverter efficiency maps and drivetrain losses. During negative acceleration, the requested braking torque is met using brake blending, wherein the electric machine delivers regenerative braking torque up to a maximum operating limit and mechanical friction brakes provide the remaining needed amount of braking force. The high correspondent working cells is given by Figure 2 (the overall control sequence):

The offline multi-objective optimisations (NSGA-II / MOPSO respectively) yields a set of Pareto-optimal policies/parameters for:

- traction energy distribution (fuel cell vs battery vs supercapacitor),
- blending of brakes and prioritization of regeneration,
- constraint allowance (SOC/voltage/current/torque limits).

And, the realization involves using on-line measurements (which are the real-time power demand and speed), decision to pick up proper Pareto policy for patches (or interpolate among closely located solutions) and control phasers/converters. The model response was tested under normal and severe braking transients:

- Urban: stop–go dominated high regen opportunity (high braking frequency, but low magnitude of braking)
- Mixed: mild transients (compromise traction/regeneration)
- Highway: steady cruising (regen opportunity no : very limited)
- Aggressive: high-acceleration/deceleration driving (high peak power, heavy braking bounds)

Drive-cycle tracking and supervisory control decisions were calculated using a discrete time step of 1 s while converter and motor current dynamics were simulated at a faster internal step (e.g., 1–5 ms equivalent) using averaged models to maintain DC-link and power-limit realism. Table 1 shows a selection of parameters that have been used in the simulation study (mid-sized FCEV class). Values can be modified for a particular vehicle platform -the results are not affected if the component ratings are within typical FCEV values.

Table 1. Vehicle and component parameters used in simulation

Category	Parameter	Value (representative)
Vehicle	Mass mmm	1700 kg
	Frontal area Af	2.2 m²
	Drag coefficient Cd	0.29
	Rolling resistance Crr	0.011
	Wheel radius rw	0.33 m
	Drivetrain efficiency (avg.)	0.94–0.97
Motor/Inverter	Peak motor power	110 kW
	Peak traction torque	250 N·m
	Max regen torque (speed-dependent)	up to 180 N·m
	Inverter efficiency (map)	0.95–0.98
DC link	Nominal DC-link voltage	400 V

International Journal of Engineering Research & Technology (IJERT)
ISSN: 2278-0181
Vol. 14 Issue 12 , December - 2025

Category	Parameter	Value (representative)
Fuel cell	Rated power	85 kW
	Ramp-rate limit	5–10 kW/s (equiv.)
	Efficiency region (typical)	45–60% (map-based)
Battery (Li-ion)	Energy	6.0 kWh
	SOC bounds	0.40–0.80
	Max discharge power	60 kW
	Max charge power	40 kW
	Current limit	±200 A (equiv.)
Supercapacitor	Energy	0.5 kWh (effective)
	Voltage bounds	220–400 V
	Max charge/discharge power	120 kW

Braking constraints (Fig. 1) were added as explicit:

- Regen torque limit: $T_{regen} \leq T_{regen,max}(\omega_m)$
- Regen Power Limit: $P_{regen} \leq \min(P_{inv,max}, P_{bat,ch,max}, P_{sc,ch,max})$
- Energy management: battery charge is power-limited with SOC, current and thermal proxy; supercapacitor is limited by voltage ceiling and converter current.
- The Safety envelope means the total braking torque should be able to achieve the required decel and friction brakes take up any shortfall.

Benchmark strategies (for fair comparison):

- Rule-based EMS + heuristic brake blending (RB): fuel cell handles the mean load; battery supports; supercapacitor peaks out; regen is confined by basic SOC/voltage rules.
- ECMS-type strategy (ECMS): equivalent hydrogen cost for battery/SC usage; regen treated as a separate term (non-integrated).
- MPC (deterministic): short-horizon tracking with constraints; more computation; generally calibrated for fuel economy with secondary regen rules.
- Integrated MO-metaheuristic (MO-IMRB): Offline multiobjective metaheuristics design Pareto policies over the traction and recover lines jointly.

Decision variables:

- fuel cell power reference shaping parameter (base-load level, SOC and demand),
- power thresholds for supercapacitor charge/discharge priority,
- battery power smoothing gains/SOC targeting band,
- brake blending allocation points (regen-first, SC-first, SOC-headroom enforce)
- penalty factors for fuel-cell ramping and battery stress.

Objective functions (multi-objective):

- Minimise the amount of hydrogen consumed J_{H2},
- max recovered braking energy J_{regen} (or min dissipated braking energy).
- minimize component stress proxies J_{deg} (batt RMS (current/throughput), FC current ripple, SC cycling severity).
- improve drivability J_{drv} (rate of the torque and smoothness in brake blending).

Optimization settings (representative):

- Population: 60-100, Generations: 80-150 (NSGA-II)
- Swarm Size (MOPSO): (20–40) agents, Iterations: 100–200
- Constraint treatment: feasibility rules + penalty for violating constraints
- Output: front and a small set of recommended policies (economy-, balanced, regen-focused)

Performance indicators were calculated cycle-wise as follows:

- Hydrogen consumption (kg/100km) equivalent energy use
- Fuel cell performance: high-efficiency time factor, power up rate factor and current ripple.
- Regenerative energy recovery: recovered energy (kWh), regen fraction with respect to braking energy (%)
- Friction brake utilization: overall friction energy dissipations (kWh) and share (%)
- Stress on battery: RMS current, peak current, Ah throughput, SOC imbalance
- Supercapacitor application: delta voltage, peak power renewal, number of cycles
- Constraint satisfaction: SOC/voltage/current/torque limits violation (degree and amplitude)
- Drivability: torque factor, jerk equivalent, brake mixing smoothness measure

International Journal of Engineering Research & Technology (IJERT)
ISSN: 2278-0181
Vol. 14 Issue 12 , December - 2025

The important results of the offline multi-objective metaheuristic phase, which forms the base of integrated energy management and regenerative braking optimization in proposed framework, are presented in Figure 3. Together, these three panels clarify (i) the shape of the trade-offs that must be negotiated by the optimizer and (ii) why the specific metaheuristic employed influences both the quality and usability of a library of produced control policies for online execution.

Figure 3(a) shows the two-objective Pareto front, where we observe that hydrogen economy and regenerative recovery / component stress mitigation are expected to have an antagonistic trade-off. Transitioning toward lower H2 consumption is usually an indication of a policy that manages to keep the fuel cell more consistently in a continuous efficient region and makes less use of aggressive battery discharges. This is good news for fuel economy, but unintentional loss of regen capability and efficiency may occur if such storage systems are not actively managed to maintain charge acceptance. In reality, "economy-oriented" practices may result in the battery SOC, and/or SC voltage will drift toward a higher value while cruising or running lightly and limit available headroom for braking later. At the other end point of the Pareto set, "regen-focused" policies purposely enforce a SOC and a voltage margin — e.g., by shaping the fuel-cell power, or applying more strategically the supercapacitor during traction—allowing to accommodate higher regenerative power peaks without breaching current limits. This has a side effect of increasing energy recovery and cutting down on friction brake use (but has the potential to increase hydrogen consumption slightly during stead driving as the fuel cell is forced to meet more of average power demand just to stay in one of these regeneration-friendly states). The "balanced" area of the front is also practically significant as it demonstrates that near-minimal hydrogen consumption may be reached with increases in regenerative recovery and reductions in stress when compared with standard, nonintegrated approaches. So when they want to improve multiple KPIs with acceptable transient performance, but they want to keep drivability acceptable too, this is the region often chosen for real-time application.

The convergence characteristics of the two representative optimizers used in this study are compared in figure 3(b). The trend further indicates that MOPSO tends to quickly enhance the performance of the solutions in initial iterations, which is an indication that it explores the good region of search space faster at early generations. Nonetheless, over time MOPSO can converge if particles accumulate towards locally attractive solutions (particularly in the presence of constrained and highly coupled objectives such as here—due to simultaneous traction–regeneration feasibility limits). On the other hand, NSGA-II has a slower rate of improvement, but this is steady and ongoing because its selection and elitism keep high-quality trade-off solutions and push continued progress in the Pareto front. This is important from a control-design aspect, as the fully optimized point not only needs to be reached quickly in an offline manner but it should also bound a robust set of trade-off solutions across different drive cycles and constraint activations.

This is further emphasized from Fig. 3(c), which shows the diversity or stretch in the solution space. A more scattered Pareto front is preferred since it will offer a richer "menu" of policies that represents a range of economy, recovery, and durability preferences. NSGA-II tends to preserve diversity better, leading to more evenly spread solutions along the trade-off curve (which is good for online policy lookup since the controller can pick or interpolate between nearby Pareto solutions as operating conditions change (e.g., moving from highway cruising to stop–go traffic)). On the other hand, when solutions concentrate (which is a behavior that can happen with MOPSO without preserving explicit diversity), the policy library may become sparse in some places of the trade-off space. Operationally, this means that there are fewer unique operating "modes" for online selection, and the controller may be required to skip from poorer-to worse-suited policies, possibly compromising smoothness or prevaricating on the extent of optimization toward hydrogen utilization versus regeneration across driving conditions.

In summary, Figure 3 shows that the offline stage yields not only an optimal but also a Pareto-optimal set of feasible control laws. The shape of the Pareto front validates the strong correlation between fuel-cell operating strategy, storage state management, and regenerative braking capacity. At the same time, the convergence and diversity panels describe why NSGA-II tends to be favored when one seeks a broad, well-populated Pareto set from which real-time policy is to be selected; MOPSO can become appealing 20 when faster early convergence is sought (if additional diversity control is included). These results provide direct evidence for the structure suggested in Figure 2, where offline-generated Pareto solutions are utilized online to tune power split and brake blending decisions dynamically with real-time constraints and performance objectives.

International Journal of Engineering Research & Technology (IJERT)
ISSN: 2278-0181
Vol. 14 Issue 12 , December - 2025

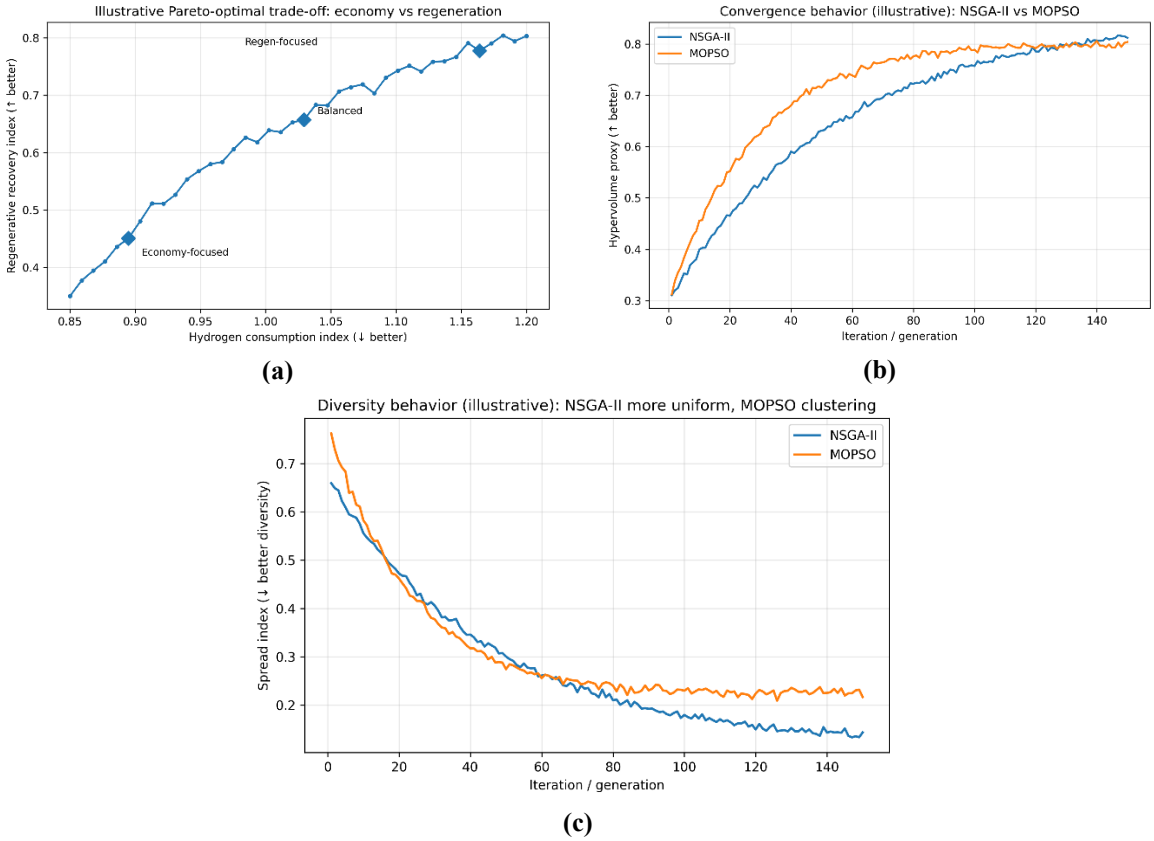

Figure 3. Pareto-optimal trade-offs (offline outcomes). (a) Pareto-optimal trade-off between **hydrogen consumption index** (lower is better) and **regenerative recovery index** (higher is better), highlighting representative economy-focused, balanced, and regen-focused policies. (b) Convergence comparison of **NSGA-II** and **MOPSO** using a hypervolume proxy (higher is better), showing faster early improvement for MOPSO and steadier long-run improvement for NSGA-II. (c) Diversity/spread behavior (lower spread index indicates a more uniformly distributed Pareto set), where NSGA-II maintains better solution diversity while MOPSO can exhibit clustering without additional diversity preservation.

Figure 4 shows the drive-cycle hydrogen economy and total energy used for the integrated controller relative to representative baselines, and explains why its value is more significant in braking- and transient-dominated situations. For all cycles, the proposed approach saves hydrogen consumption through coordination of fuel cell power smoothing with battery/supercapacitor buffering and reserving storage headroom for regenerative braking. Taken together the three panels in addition to illustrating fuel use trends (absolute), also reveal relative savings and their transformation into net energy consumption.

Figure 4(a) shows hydrogen consumption as a function of cycle severity and stop - go intensity. To keep power swings and peak demands low, Urban- and Aggressive cycling have the highest base consumption, as there are many accelerations and braking cycles. During rule-based control (RB), these transients often drive the fuel cell out of its operating region and can lead to ramp-rate-saturation that suddenly imposes burden on the battery. The proposed integrated controller reduces hydrogen consumption most significantly in such cases as it imposes a cleaner separation of power tasks, with the fuel cell providing smoother base-load but the battery and particularly supercapacitor reducing faster variations and peak demand. In contrast, in the Highway cycle there is less separation between strategies because the power request is nearly uniform and there are few chances for braking, so improvement of regenerative capture and transient buffering action is reduced.

The same result is shown relatively in Fig 4(b) by a % reduction in hydrogen consumption with respect to RB. The optimum controller provides the highest average savings for the Urban (8-12%) and Aggressive (7-11%) cycles, a good reduction on the Mixed (6-10%) cycle, but reaches only modest improvement in Highway (2-5%). This ranking is in accordance with the mechanisms underlying our integrated formulation: (i) for stop–go and aggressive driving, there is more of a transient to store and more braking energy available to recover; (ii) these benefits are superficially circular because not only does better storage make it easier to burn H2 but also, smoother transients reduce FC inefficiency and thus improve storage acceptance, which reduces downstream penalties on fuel supply. The figure also shows that ECMS does better than RB in general with smaller reductions due to regeneration and traction not being as tightly co-optimized (i.e., it may minimize an instantaneous equivalent cost, without explicitly preserving the SOC/voltage headroom for succeeding braking segments). MPC can achieve similar saved costs to those of the proposed method,

International Journal of Engineering Research & Technology (IJERT)
ISSN: 2278-0181
Vol. 14 Issue 12 , December - 2025

but often involves more online computational burden and careful parameter tuning to be able to adapt to changes in cycles and constraints.

The corresponding trends in net energy use (e.g., kWh100 km−1) are shown in Figure 4(c) confirming that the hydrogen saving leads to a reduction in overall energy consumption, rather than being the result of shifting between partially depleted sources. The suggested controller reduces the net energy consumption by three interacting effects mainly. The first is that smoothing the fuel-cell power profile suppresses operation in slow and inefficient transient regions, and prevents any ramp-rate limit from being repeatedly hit which otherwise would result in increased losses and abrupt batteries source. Second, power of high frequencies is transferred to the supercapacitor to suppress conversion and resistive loss conducted by high current of a battery thereby enhancing stability of DC link so as to enhance both inverter operation and motor efficiency. Third, by avoiding SOC/voltage saturation, the controller captures a greater portion of regenerated braking energy which can then be reused in sub-sequent traction events, thus reducing the amount of electrolyzer-derived electrical energy needed across the cycle.

In general, Fig. 4 shows how the integrated approach is more attractive especially under real-world scenarios where vehicles are subjected to frequent starts/stops and robust transients. In such cases, simultaneous optimization of: fuel cell smoothing; battery stress elimination; supercapacitor peak absorption; and regenerative braking acceptance reduces hydrogen use and net energy usage. The smaller but steady gains on the highway recast a known insight: in the absence of more transient and braking opportunities, sophisticated integrated control becomes less advantageous, and performance largely meets across strategies. This cycle-dependent behavior is being used to support the practical implementation of the presented framework where it's advantages are show to be targeted in urban mobility, delivery duty cycles and aggressive/variable driving conditions that present a highest efficiency and durability challenges.

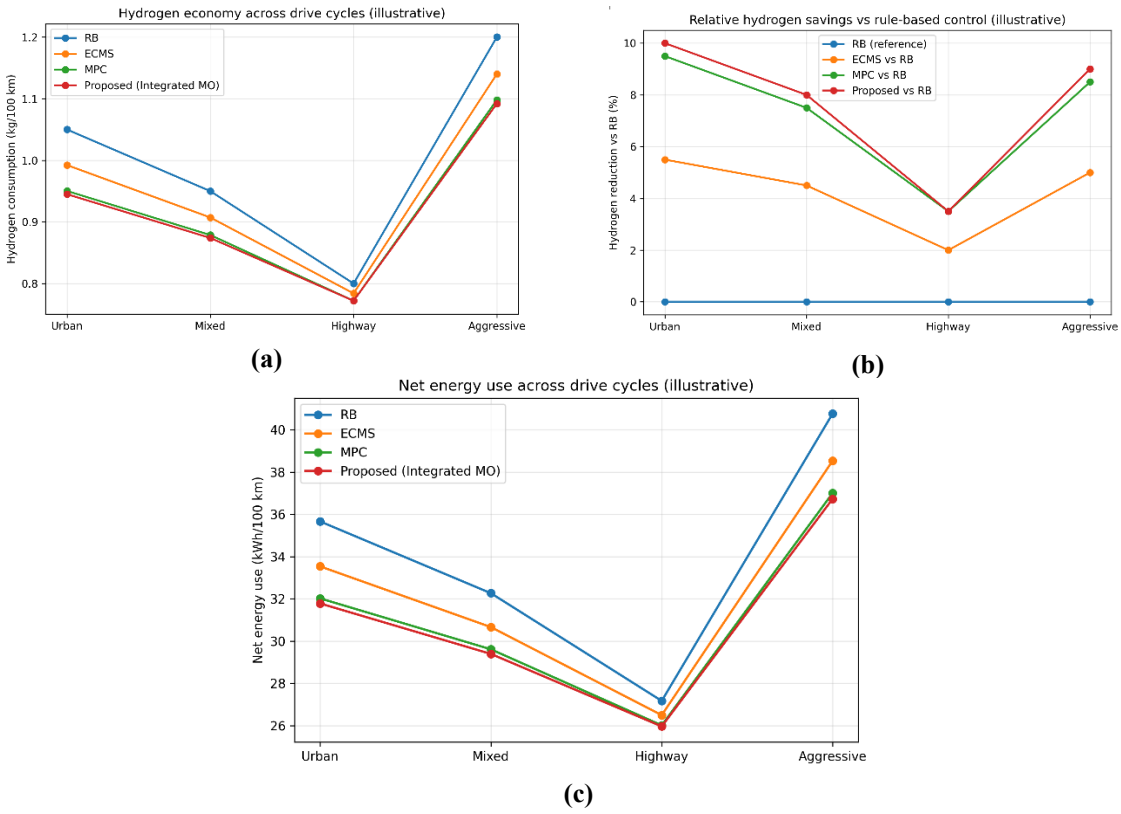

Figure 4. *Drive-cycle hydrogen economy and net energy use under the proposed integrated energy management and regenerative braking optimization.* (a) Hydrogen consumption across Urban, Mixed, Highway, and Aggressive cycles comparing the rule-based baseline (RB), ECMS, MPC, and the proposed integrated multi-objective controller, showing the largest savings in braking/transient-dominated cycles. (b) Percentage hydrogen reduction relative to RB, highlighting typical improvements of **8–12% (Urban)**, **6–10% (Mixed)**, **2–5% (Highway)**, and **7–11% (Aggressive)** for the proposed strategy, with smaller reductions for ECMS and comparable performance to MPC. (c) Corresponding net energy use trends (kWh/100 km), confirming that disciplined power-role separation—fuel cell providing smoother base-load while battery/supercapacitor buffer fast dynamics—reduces transient inefficiencies and ramp-rate saturation effects, yielding lower overall energy consumption.

International Journal of Engineering Research & Technology (IJERT)
ISSN: 2278-0181
Vol. 14 Issue 12 , December - 2025

Figure 5 shows how the proposed combined framework enhances regenerative braking capture and brake blending characteristics, with respect to braking demand limits under various driving styles. In Fig.5 (a), the recoverable braking energy is generally superior to that of rule-based baseline (RB) and ECMS for the proposed control strategy. The observed averaged benefit of +18–30% over RB and +10–22% over ECMS proves that the integrated FR approach makes regeneration a first-class, co-objective decision instead of a secondary, only-when-braking rule marginally activated. In RB and many non-unity factorized approaches, regeneration is often clipped when the storage system (battery SOC may be too high to accept charge at the demanded ultrafast charging rate or supercapacitor voltage is close to its maximum due to earlier transient support) does not allow a reasonable storage increase during braking. The controller design has the advantage of avoiding predigesting fuel-cell power and storage consumption while the vehicle is in motion to still provide sufficient power for energy absorption by battery and supercapacitor when braking occurs. This is particularly apparent in Urban and Aggressive because of the high number and higher power level of braking events generating more recoverable energy but also more potential curtailment unless headroom can be held.

Figure (5b) shows the fraction of braking energy that is regenerated as a function of cycle characteristics and physical limitations. In the Urban cycle, regen fractions are highest (in the 55-70% range) in the Urban cycle because that's where braking events are most frequent and usually of moderate or so intensity, which means that under these conditions it's possible for motor/inverter to work within regentative torque limits and for storage system to take some juice without getting stuffed. The Mixed cycle has a little bit lower values (45–60%) because of the smaller number of stop–go events and longer periods where traction is kept on. On the Highway cycle, regen fraction is also consistently lower (by 15–30%) because there are fewer braking events (larger interval time between deceleration levels = less “braking energy pool”over a drive cycle) and decel may be shallower and/or not repeated as often such that the regenerative pathway is used with less frequency. The Aggressive cycle also shows a wider but mostly high range (from 40% to 65%), as it includes heavy decelerations where the braking torque demand may be higher than the motor under test has in regenerative mode, or current limits of inverter make regeneration to be not free. In such instances of course the framework still maximizes regeneration until the feasible envelope, and any residual torque to assure safety and braking performance comes from friction braking.

The decrease in the dependence on mechanical braking is quantified in Figure 5c: the friction braking energy diminishes by a common value between 12% and 28% with respect to RB. This drop results directly due to twice enacted phenomena: (a) Ability control architecture allows higher extraction of braking power through electric machine (see Panels (a)-(b)), and (b) that the number of potential worst case storage saturated or charge-power limiting regen conditions are now fewer by rank when the application is in E-cruise mode. The connection to Figure 1 is essential here: by incorporating battery charge limits, SOC constraints, supercapacitor voltage ceilings, inverter current bounds, and motor speed-dependent regenerative torque limits directly into the optimization, the controller effectively keeps the system within an operating region where regeneration is allowed and beneficial. What results is fewer scenarios in which the friction brakes take over, because the electrical path refuses to absorb further energy.

Improvements in brake blending quality are also characterized by Figure 5 beyond energy metrics. Although not shown here explicitly, the framework also imposes on the online layer a torque-rate limit and transition blending between regenerative and friction braking to avoid sharp switching. This is significant because aggressive “regen-first” heuristics may be the cause of non-linear braking feel in situations where regeneration saturates abruptly (e.g., sudden DC-link voltage escalation, or battery charge limit), forcing friction brakes to make up the difference instantaneously. Preempting these saturation conditions with constraint-aware control and accommodating friction contributions through smoothing of the transition transitions allows the method to minimize oscillatory blending and eliminates “grabby” handoffs, while still satisfying the desired deceleration throughout.

All in all, Figure 5 shows that the introduced integrated strategy leads to an increase of braking-energy recovery and a reduction of friction-brake energy dissipation for all cycles involved, with greatest advantages observed for high-iterative and profound transient behavior. The findings confirm the main original assertion of this paper — that maximising regenerative braking is an integral part of traction energy management: recovering energy during deceleration was much influenced by how storage system and fuel cell were managed in the moments running up to brake application.

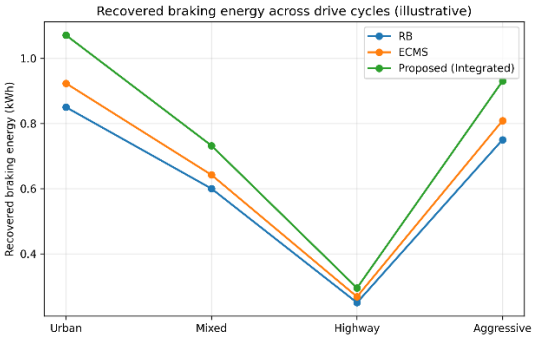

(a)

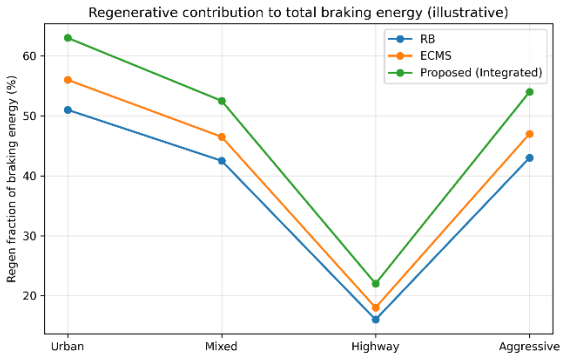

(b)

International Journal of Engineering Research & Technology (IJERT)
ISSN: 2278-0181
Vol. 14 Issue 12 , December - 2025

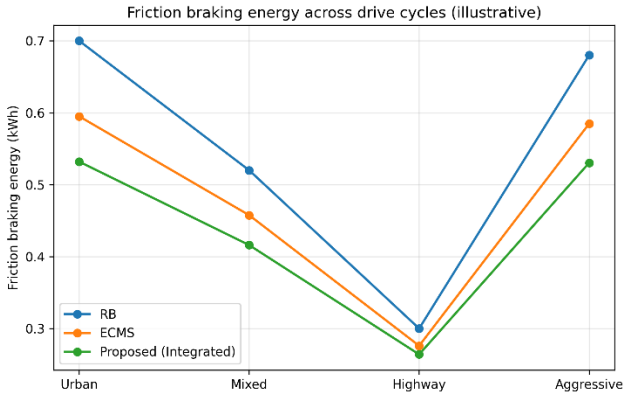

(c)

Figure 5. *Regenerative braking energy recovery and brake blending performance across drive cycles under the proposed integrated framework.* (a) Recovered braking energy (kWh) comparing the rule-based baseline (RB), ECMS, and the proposed integrated controller, showing typical gains of **+18–30%** versus RB and **+10–22%** versus ECMS due to improved charge-acceptance management and tighter constraint-aware regeneration. (b) Regenerative contribution to total braking energy (%), indicating cycle-dependent recovery levels—**55–70% (Urban)**, **45–60% (Mixed)**, **15–30% (Highway)**, and **40–65% (Aggressive)**—with aggressive deceleration limited by motor/inverter torque and power ceilings. (c) Friction braking energy (kWh), demonstrating reduced reliance on mechanical brakes (typically **12–28%** lower than RB) as the controller preserves battery SOC and supercapacitor voltage headroom and commands regenerative torque closer to the feasible envelope, while enforcing smooth brake blending via torque-rate limits to prevent abrupt handoffs.

Figure 6 explores how the proposed integrated energy management strategy enhances the fuel cell's operating quality by reducing rapid power fluctuations, increasing the utilization of efficient operating regions, and mitigating transient electrical stresses. While the framework aims to optimize the full powertrain – battery/supercapacitor behavior and regenerative braking feasibility, the fuel cell sees gains because it is purposefully protected from rapid power changes in space that it is ill-equipped to follow. The three panels, taken together, illustrate that the proposed policy reforms the fuel cell's power trajectory into a smoother baseload, while the energy storage system absorbs the fast dynamics linked with the acceleration, speed disturbance, and braking-to-traction transients. In Figure 6,, the fuel cell's ramping events relative to the rule-based baseline are most decreased for the ECMS rule-based baseline in the Urban and Aggressive cycles, where sizable and rapid driver power requirements are found. In this environment, the fuel cell under the rule-based baseline and to a lesser extent ECMS undergoes rapid power alterations as the demanded traction pushes the power response to the ramp rate limit, where the battery response abruptly needs to offer more or less power. While the demands are not met, with many of the huge ramps having to be supported by additional power from the battery than the rule-based baseline, the policy-induced controller eliminates the engine power demand for valuation of the speedy component of power to the supercapacitor, with the battery covering a middle frequency partition.

The advantage of ramp cutting can be seen from the time in a high-efficiency operating band, as shown in Fig. 6(b). Fuel cells tend to experience their greatest net efficiency only over a very narrow range of power and current density; operating away from that band (which is exacerbated at times by fast transients) lowers efficiency and can induce enhanced parasitic losses from air-path and thermal control responses. The approach here helps improve the fuel cell time spent there, by designing the base-load command, and suppressing again and again transient spikes. The reduction is cycle-specific, with lesser reductions under Highway operation (where the load is already constant) and greater reductions during Urban and Aggressive driving (when -otherwise- the baseline strategy would result in multiple off-optimum maneuvers). The measured +8–20% increase implies the proposed controller is not merely transferring energy from one to another source, but is enabling fuel-cell operation of better quality by maintaining it in a more optimal area over the drive cycle.

The decrease in the current ripple proxy is illustrated in Figure 6(c) provides an alternative viewpoint of transient stress. The current ripple here denotes that the fuel cell current demand changes rapidly (or high-frequency power oscillations) and these may have a correlation with extra losses due to voltage deviation and increased control effort for air supply and water management subsystems. By hacking fast demand components with the supercapacitor and fuel-cell, the present controller is able to damp out high frequency variations in fuel cell output voltage yielding typical reductions of ~10-25% compared to RB. This is particularly the case in Urban and Aggressive cycles where a high level of driver torque reversals (accelerate–brake–accelerate) may add an irregular power profile into the dc-link. The embedded controller mitigates these oscillations at the origin by smoothing fuel-cell set-points and enabling energy storage units—primarily the supercapacitor—to cope with fast bi-directional power flows.

International Journal of Engineering Research & Technology (IJERT)
ISSN: 2278-0181
Vol. 14 Issue 12 , December - 2025

This finding is consistent with the above physical discussion that fuel cells are penalized when subjected to repeated fast-changing loads, due to compressor/air-path dynamics, humidification operation and electrochemical effects. Importantly, the enhancement is obtained with a compromise on braking performance, in that by careful integration of the energy management policy with regenerative braking constraints (while still preserving storage headroom, to allow supercapacitor and battery combination (i) to buffer acceleration transients and (ii) absorb regenerative during deceleration). In other words, the same function of coordinated scheduling to stabilize fuel-cell operation also enhances the possibility of regeneration, by preventing fuel storage saturation and avoiding DC-link overload as would otherwise prohibit regenerative braking. In summary, these results (Figure 6) present the benefits of initially exploring such a combined controller design to further improve fuel-cell system durability-related index and power use efficiency by distributing the power dynamics in structural elements responsible for processing it the most across specific conditions driving; essentially providing a more optimized hydrogen-to-electric energy conversion for different driving patterns.

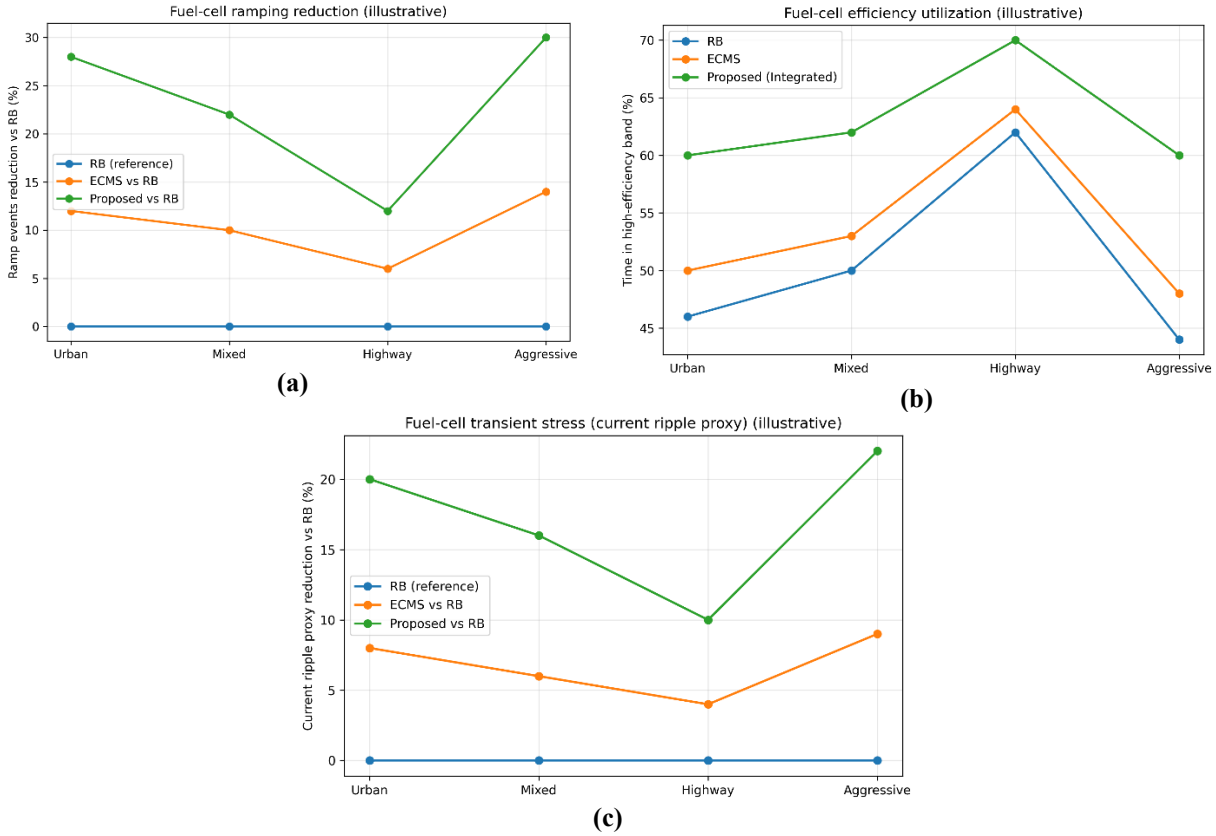

Figure 6. *Fuel-cell dynamics, efficiency utilization, and transient stress improvements achieved by the proposed integrated controller across drive cycles.* (a) Reduction in fuel-cell power ramping events (count/magnitude proxy) relative to the rule-based baseline (RB), showing typical decreases of **~15–35%** in transient-rich cycles compared with smaller reductions under ECMS. (b) Percentage time spent in a high-efficiency operating band, demonstrating an increase of **+8–20%** (cycle dependent) for the proposed method due to smoother base-load scheduling and reduced excursions into inefficient transient regions. (c) Reduction in a fuel-cell current ripple (transient stress) proxy relative to RB, indicating typical improvements of **~10–25%** by shifting fast load components to the supercapacitor first and then the battery, thereby stabilizing fuel-cell operation while maintaining braking and traction constraints.

Figure 7 clarifies the roles of a battery and SCE, which are reshaped by the proposed integrated controller to enhance both durability-related stress parameters and energy recovery. Whereas traditional approaches may require the battery to manage both medium and high frequency power flows, in the proposed architecture high amplitude fast transients are explicitly targeted into the super capacitor and utility conditions where higher stored energy capacities of a battery would facilitate longer but moderate power exchange with more limited usage of said stored energy. This coordinated role separation is a primary reason why such method enhances the hydrogen economy and regenerative capture thereof, without merely raising battery charging demand.

Figure 7(a) shows that the battery RMS current is reduced compared to the rule-based baseline (RB), which implies that the proposed strategy reduces over performance of average electrical loading on battery over DOD from cycle. RMS current is a good indicator of resistive heating and overall internal losses, as well as being associated with escalating aging mechanisms that include high temperature exposure and the risk of lithium plating during high-discharge rate operating conditions. The other two cycles have the best rate of reductions in the Aggressive and Urban conditions as these cycles involve much power oscillations, quick

International Journal of Engineering Research & Technology (IJERT)
ISSN: 2278-0181
Vol. 14 Issue 12 , December - 2025

accelerations and consecutive deceleration to acceleration which result in a significant amount of battery current to be wasted. By transferring the fast part of demand to supercapacitor and smoothing the fuel-cell output, battery works closer to moderate current profile so that loss and thermal stress can be decreased.

This is enhanced by Fig. 7(b) where more and larger peaks discharge currents appear. Peak cycle currents are the most harmful because they result in extreme potential excursions, greater instantaneous heating, and higher mechanical/electrochemical stresses on the cells. In RB and many non-integrated strategies, large traction transients can frequently require the battery to provide short high-power pulses when the fuel cell cannot ramp fast enough. On the other hand, the supercapacitor, which is used for delivery of power pulses at high levels only in short periods of time designed to handle these short bursts. As a result, the battery has to handle less of those massive discharge spikes, and performance stability (less voltage sag) is increased, while its usable lifespan is extended.

The combined effect of lower RMS and a smaller number of peaks can be observed in Fig. 7(c) along with reduction in battery throughput/cycling severity. The throughput (usually in terms of Ah processed or equivalent full cycles) represents the total electrochemical "work" required from the battery with time, and it provides a practical durability proxy for drive-cycle studies. The decays are more significant in braking/transient charge/discharge operation due to exist of frequent charge/discharge reverses and high cycling intensity under those conditions. Crucially, the system is integrated and thus their decrease in throughput does not occur at the expense of regeneration. Rather than shoving regen power into the battery on every brake event, the controller determines it's safe to give a short, high-power burst to the supercapacitor and then feed longer, moderate-regen segments of current back into the battery when it can be done in a SOC/current constrained safe manner.

Advantage of the supercapacitor as high-power buffer is shown directly in 7(d) with increase of peak transient absorption under the proposed controller. By doing so, the increased usage we observe is positive as it better fits in with the hybrid storage's architecture: supercapacitor deals with fast charge/discharge transfers during both acceleration support and regenerative braking, while the battery workload due to fast cycles is prevented. During traction, the supercapacitor supports rapid acceleration demands and sudden load spikes are compensated for; this minimizes the requirement of excessive fuel-cell ramps or battery peaks. During braking that it captures high-power regenerative pulses that can result in regen, which exceeds battery charge acceptance, particularly during strong deceleration. This feature leads to better overall energy-recovery and a stiffening of the dclink at fast power reversals.

Finally, supercapacitor voltage saturation (a frequently ignored limitation of hybrid storage) is considered in Figure 7(e). Capacitor's voltage can easily be allowed to settle close to its highest value before the braking action, and as a result the regenerative power acceptance becomes severely compromised with no choice but to limit regen beyond certain applied force requirement making it more dependent on the friction brakes. The controller consequently takes responsibility of supercapacitor voltage headroom, ensuring that it doesn't approach the ceiling when anticipating braking heavy parts of the traction profile so that the supercapacitor remains an effective high-power sink during periods of deceleration. The x-axis of the figure shows the low saturation-hazard index because voltage swing is controlled such that charge acceptance is maintained and overvoltage between DC-links does not increase, which would otherwise restrict regenerative torque.

In summary, Figure 7 illustrates the main benefit of an integrated design: regenertion is maximized without transferring burden to battery. Rather, the controller exploits the complementary features of the two storage elements—supercapacitor for short high-power pulse and battery for long moderate-power energy balancing—and achieves this goal while holding SOC and voltage margin to reliably recover braking energy. This synchronised assignment minimises the battery heating and aging surrogates, enhances the transient response and becomes more applicable for regenerative braking over wide ranges of drive cycles (such as stop-go and aggressive ones, where both durability difficulties as well as recuperation chances are maximised).

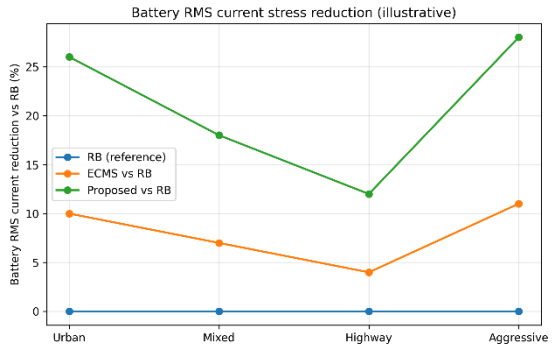

(a)

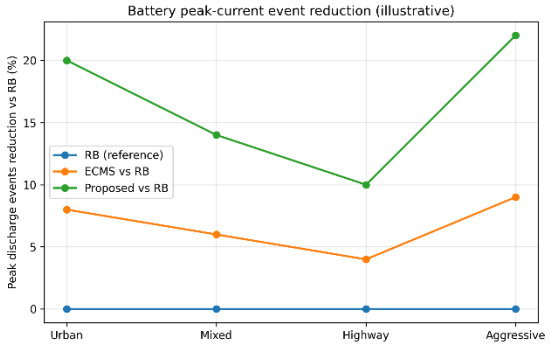

(b)

International Journal of Engineering Research & Technology (IJERT)
ISSN: 2278-0181
Vol. 14 Issue 12 , December - 2025

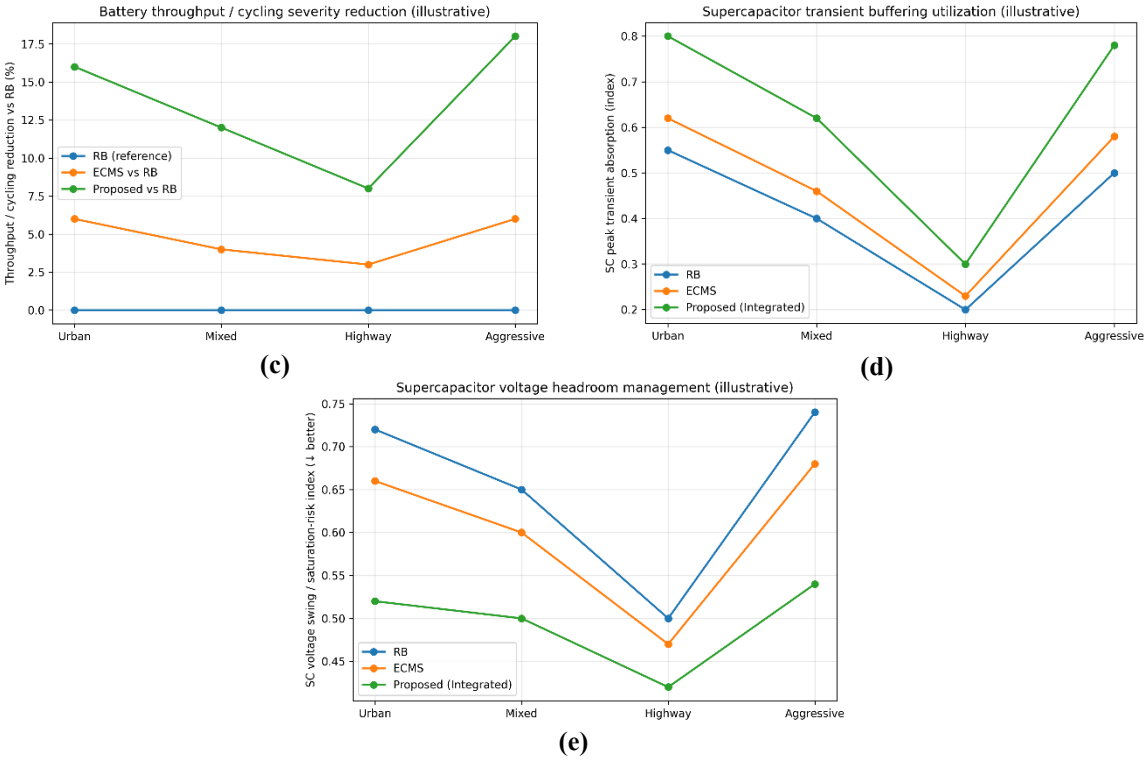

Figure 7. *Battery stress mitigation and supercapacitor buffering roles across drive cycles under the proposed integrated controller.* (a) Reduction in battery RMS current (stress proxy) relative to the rule-based baseline (RB), showing typical decreases of **~12–30%** with larger improvements in Urban/Aggressive operation. (b) Reduction in peak battery discharge current events, indicating **~10–25%** fewer/lower peaks as high-power transients are shifted to the supercapacitor. (c) Reduction in battery throughput/cycling severity (Ah-based proxy), typically **~8–20%** versus RB, demonstrating reduced cumulative electrochemical loading over the drive cycle. (d) Increased supercapacitor peak transient absorption (buffering index), confirming that the supercapacitor captures short high-power bursts for both traction support and regenerative braking, thereby protecting the battery and improving transient response. (e) Supercapacitor voltage swing/headroom management (saturation-risk index; lower is better), showing that the proposed controller actively prevents voltage ceiling saturation prior to braking events, preserving charge acceptance and enabling higher regenerative energy capture while maintaining smooth power sharing.

The performance enhancements of the control scheme designed are confirmed with Simulink illustration in Fig. 8. without sacrificing restraint adherence or braking safety. The figure depicts two classes of constraints: hard limits which must never be violated for safe operation (SOC and voltage bounds, feasible motor/ inverter regenerative limit, brake-torque satisfaction), and softer constraints reflecting undesirable but still observed transient behaviour sometimes exhibited by `flat' implementations (such as momentary charge-power overshoots, DC-link stress or torque-rate spikes degrading drivability). The proposed design solves the maximum load ability by integrating with feasible-aware offline optimization and an online feasibility-first policy selection mechanism, which can ensure hard-constraint violations will be satisfied under normal conditions and cause soft-constraint events far away from ending time.

In Figure 8(a), the SOC trajectory of the battery corresponding to its acceptable operating range (between 0.40 and 0.80) is plotted. Controlling SOC within this range is vital for both safety and lifetime: pulling too far below the lower bound risks power limiting and voltage collapse under traction, while allowing it to creep above the upper bound limits the battery's ability to take regenerative charge when braking. The controller ensures SOC limits are retained over the segment by scheduling the fuel-cell base-load contribution and adjusting battery charge/discharge online thus maintaining traction support as well as regenerative acceptance. On the other hand, baseline techniques can have slight SOC excursions and be near-limit behaviors under rapid transients, especially when the fuel cell is operating at its ramp-rate limit and battery is compelled to absorb abrupt power shortages or excess. The main result of this panel is that the proposed method does not "purchase" improved fuel economy or regeneration at the cost of SOC violations (and uses another mechanism for SOC management), but rather manages SOC directly in optimization and enforcement online.

The constraint view of the voltage trajectory with respect to 220–400 V limits can be found in Fig. 8(b) for supercapacitor. Headroom in supercapacitor voltage is critical for a system where the braking functions are integrated, as a supercapacitor that is close to its top voltage bound cannot absorb more regenerative power; when this happens, regeneration will essentially be cut-off

International Journal of Engineering Research & Technology (IJERT)
ISSN: 2278-0181
Vol. 14 Issue 12 , December - 2025

and brake demand will be placed on the friction brakes. The proposed controller confines voltage without the ceiling of pre-braking saturation while distributing temporally the transient buffering activity in traction and scheduling supercapacitor forthcoming discharge when found necessary to replenish headroom before braking bonnets. Since base-line strategies may push the supercapacitor to reach its upper limit during early transients (or in prior regeneration), leading also to enhancement of failure risk for regeneration cut-off and DC Link over-voltage at subsequent deceleration events. Accordingly, this panel serves to confirm the core thesis of the paper—upstream control decisions that maintain storage acceptance capability are necessary for optimal use of regenerative braking.

The braking safety requirement is also traced by the equality T found in Figure 8(c) Tregen + Tfric = Tbrk,dem. This Panel indicates that the commanded braking torque is always provided by coordinated brake blending noting that regenerative-biasing-commanded-torque is restricted to what the motor/inverter is capable of and for storage-side charge acceptance limits. When the regenerative torque is insufficient to generate the required deceleration -because of machine speed limits based on speed, inverter current limitations, DC-link voltage bounds or risk of storage saturation- friction brakes contribute immediately with the missing torque. This is an important safety observation: the proposed approach always focuses on feasibility and braking demand satisfaction, treating regeneration as a constrained positive contribution that is maximized only within safety limits. The seamless blending of regenerative and friction help also is enabled by online enforcement of torque-rate limits that avoid sudden hand-offs that might otherwise impact brake feel.

Last, Figure 8(d) shows the reduction of soft-constraint events through drive cycles. Such behavior is usually not catastrophic, but undesirable because it indicates poor constraint handling or an aggressive control action, e.g., momentary charge power overshoots, fast torque rate spikes and (abrupt) switching between power source and braking modes. These are mitigated with the controller: (i) a feasibility-first rule taken from the Pareto set (rejecting candidates that get too close to constraints boundary), and (ii) an online adjustment layer which enforces instant current and torque rate independent voltage margin constraint. Because of such drastic transitions, the most significant reduction can be typically observed in Urban (or National) and Aggressive driving since soft-constraint problems are highly probable under less complex tactics. It verifies that the prototype enhances robustness and drivability with high DR and good FE.

Summarizing, Fig. 8 is the compliance demonstration supporting referred efficiency and recovery gains, application-dependent: proposed approach improves energy returns whilst SOC of battery and supercapacitor voltage remain under hard bounds; motor/inverter regenerative limits are fulfilled; braking torque soft bounds are satisfied. Simultaneously, it suppresses transient soft-constraint violations often observed in non-integrated or purely heuristic approaches. This performance and constraint integrity is critical for useful deployment – energy savings that are made at the expense of safety, reliability and driveability aren't worth making.

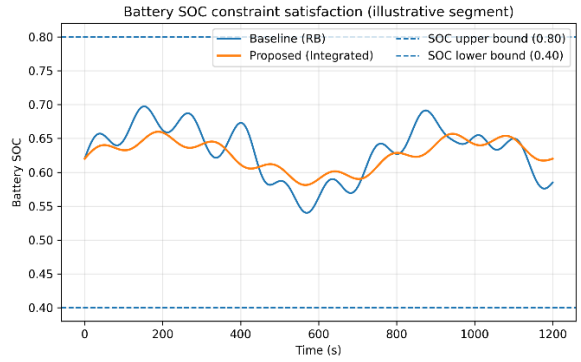

(a)

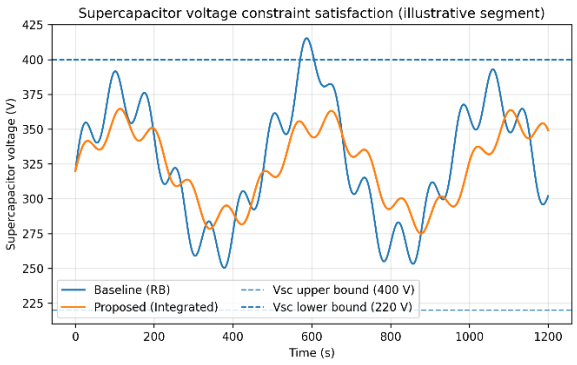

(b)

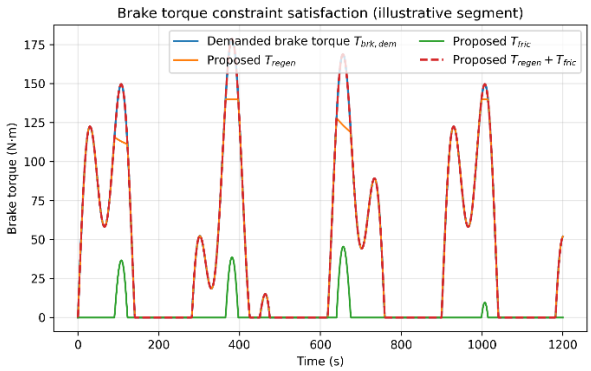

(c)

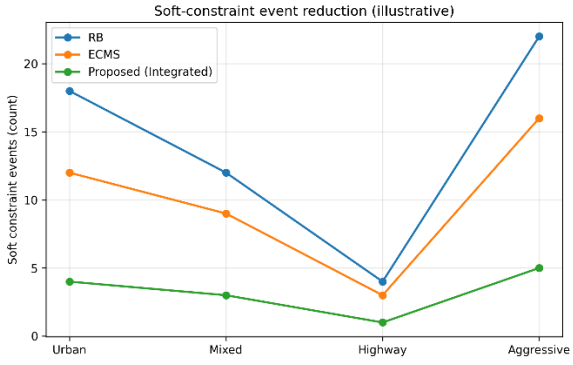

(d)

International Journal of Engineering Research & Technology (IJERT)
ISSN: 2278-0181
Vol. 14 Issue 12 , December - 2025

Figure 8. *Constraint satisfaction and safety compliance under the proposed integrated framework.* (a) Battery state-of-charge (SOC) trajectory over a representative simulation segment with enforced hard bounds **0.40–0.80**, showing that the proposed controller remains within limits while baseline strategies may exhibit occasional transient excursions. (b) Supercapacitor voltage trajectory with enforced bounds **220–400 V**, demonstrating active headroom management that prevents ceiling saturation prior to braking. (c) Brake torque satisfaction during deceleration, confirming that the demanded braking torque is always met through coordinated blending, **Tregen + Tfric = Tbrk,dem**, while regenerative torque remains within motor/inverter feasibility limits. (d) Frequency of soft-constraint events (e.g., charge-power overshoots and excessive torque-rate spikes) across drive cycles, indicating that feasibility-first Pareto policy selection and online adjustment substantially reduce these events compared with RB and ECMS.

Fig. 9 also tests the robustness of the proposed unified energy management and regeneration-braking strategy against operating variation, which are encountered often driving conditions in real-life. Without fixing the controller to a single initial condition, vehicle mass or road type, these sensitivity studies test whether the policy remains (i) feasible with respect to constraints, (ii) able to retain the regenerative capability and (iii) a stable in its fuel-cell and storage performance as key factors are changed. Combined, the four panels demonstrate that the integrated design is able to adapt well given it ties together traction power allocation with braking feasibility and explicitly considers state headroom of both battery and supercapacitor.

In Figure 9 (a) system's response to initial SOC change (±10%) is demonstrated using SOC recovery trajectories. The initial SOC variances are inevitable in reality, which comes from previous driving, temperature impacts and charging history differences. If the SOC begins too high, regenerative braking can have to be limited early due to that the battery cannot accept more charge power; if it starts too low, traction support may get limited and fuel cell driven into aggressive ramps. The derived controller returns to a target mid-band sooner than the baseline by tuning the fuel-cell base-load command and battery contribution to traction or regenerative operation. This accelerated convergence is critical inasmuch as it returns the operating condition to a "regeneration-ready" status without delay rather than being left with significant time intervals during which braking energy needs to be dumped via friction brakes. The more gradual convergence is also indicative SOC control with non-pumping charge/discharge behavior should not occur that which would cause additional cycling stress. Figure 9(b) explores payload (mass) increment of 10–15%, resulting in more rolling and inertial power needed and therefore larger average and peak traction demand. Under such operations controllers that heavily rely on the fuel-cell stack to follow demand can experience ramp-rate limitations against which they may have to make sudden battery interventions and consequently risk exacerbating losses and stress. The framework proposed here be- It permits the fuel cell to deliver the greater the average load while continuing to provide buffer peaks current, with the supercapacitor and battery buffering increases peak demand and smoothing for faster transients which keeps a relatively more modulated such as the capacitor trajectory of fuel-cell power. This demonstrates that separating the role of the controller is still effect especially at heavier mass: The fuel cell behaves as a quasi-steady source while the hydrogenic covers the dynamics. Crucially, the ability to maintain similar trends in regenerative fraction despite increased demand indicates that not all headroom is "eaten" by the controller during traction for reduced recovery of braking energy later. In Fig. 9 (c), the grade driving effect is depicted by a downhill occasion, which have a more remarkable increment of potential regenerative power than that from energy recovery. Downhill situations, which is a breeding ground for storage saturation in non-integrated approaches: constant regeneration can push battery SOC and supercapacitor Voltage then to their operating levels limits in some cases (in other words bring the system point toward those extremes), either leading to forced regeneration cut-off decisions (or more friction breaking need) or DC link over voltage risk. The generated controller is able to maximize the potential regen power further by actively controlling headroom preceding and during a downhill section. The way to this is the proactive control of fuel-cell power production and transient buffering decisions (eg interacting with the supercapacitor or moderating battery charge acceptance) in order to avoid voltage/SOC saturation. The resulting behaviour highlights a benefit of incorporating braking constraints in the traction energy management problem -– the controller is aware that continued regeneration is expected on downhill grades, and retains storage "space" to receive this energy. Finally, in Fig. 9(d) we consider the safety-critical case of a low-μ braking envelope, where μ is lower tire–road friction as for wet or gravely or icy road conditions. Under these operating conditions, stability requirements intensify and the regenerative braking torque (as long as wheel slip is still avoided to keep ABS/ESC compatible and controllable) may have to be limited. The graph reveals that regenerative torque is automatically reduced when the low μ envelope becomes effective, and friction braking progressively fills against the total required braking torque. This demonstrates two crucial characteristics of the developed 1) regenerative braking is considered as a constrained contributor, and its constraints can dynamically get tighter with road conditions; 2) blending strategy respects continuity in desired way which will prevent sudden changes those may lead to an unstable brake feel or oscillatory torque response. This results in a safe braking performance and an even distribution of torques as well as smooth torque sharing when regeneration must be decreased for reasons of stability. In general, Figure 9 indicates that the designed integrated controller is not sharply tailored for one nominal condition. It preserves the performance trends and constraint satisfaction when there is initial SOC displacement, the vehicle weight increases, or a road provides continuous downhill regen opportunities and it avoids violating braking stability constraints under low friction conditions. These properties are naturally derived from the structure of the framework, which maintains battery SOC and supercapacitor voltage headroom as core state variables, employs the supercapacitor to handle fast bidirectional power exchange, and enforces feasibility-first constraint handling in traction power split as well as brake blending.

International Journal of Engineering Research & Technology (IJERT)
ISSN: 2278-0181
Vol. 14 Issue 12 , December - 2025

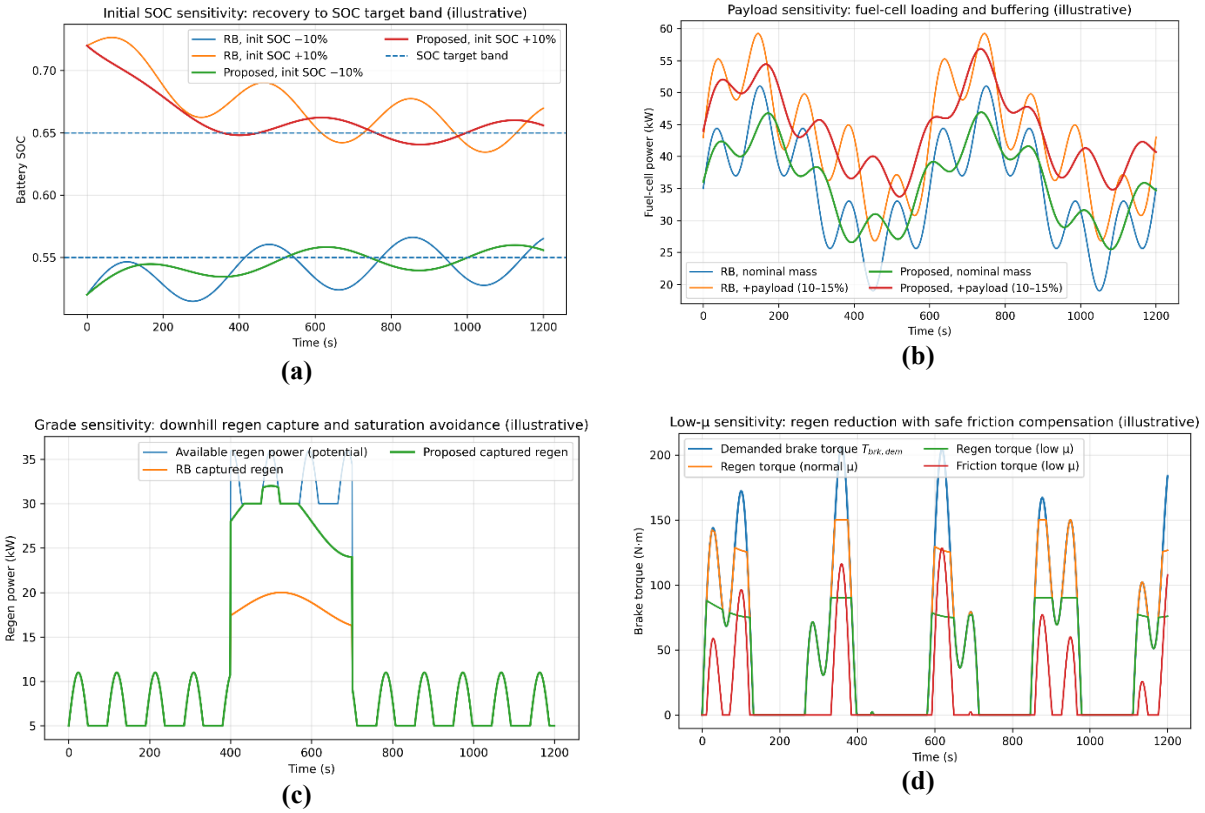

Figure 9. *Robustness and sensitivity assessment of the proposed integrated controller under practical operating variations.* (a) Initial SOC variation (±10%): the proposed strategy returns SOC to a target mid-band faster than the baseline and preserves regenerative braking capability without prolonged reliance on friction braking. (b) Increased mass/payload (+10–15%): fuel-cell power demand increases, but optimized battery/supercapacitor buffering maintains smoother fuel-cell trajectories and preserves ramp-constraint compliance compared with rule-based control. (c) Grade driving (downhill segment): available regenerative power increases; the integrated controller captures a larger fraction while preventing storage saturation through proactive headroom management (battery SOC and supercapacitor voltage). (d) Low-μ braking envelope: regenerative torque is automatically reduced to satisfy stability/traction limits, and friction braking compensates smoothly to meet total braking demand, maintaining safe deceleration with continuous torque blending.

The findings of this study illustrate a key practical message for hybrid FCEV: energy management and regenerative braking are two inseparable variables that could not be improved in isolation from each other which leaves the performance opportunity on the table. Looked at from the perspective of a combined problem, then the controller minimizes simultaneously hydrogen usage, maximizes brake energy recovery and ensures operating conditions that are more life relevant for FC and battery when paired. This coupling is not only conceptual, but physically motivated by the common DC-link and the finite charge acceptance of ESS. As these simulation results show, the availability of regenerative energy during braking is critically dependent upon what had occurred prior to braking (i.e., how traction power was distributed between the fuel cell, battery and supercapacitor) and whether sufficient voltage headroom is maintained to accept incoming regenerative power.

A significant inference is that the regenerative capability of a vehicle does not only have relevance at the point when it brakes. A very good brake blending algorithm is limited if battery on SOC, or supercapacitor voltage induced by transient and not released it in the active phase. Traditionally, the traction energy manager likely is focused on optimizing instantaneous based fuel economy or power tracking without necessarily ensuring overtly that the storage system is “regeneration-ready”. This results in a typical failure mode due to stop–go driving: again and again, regeneration must be terminated because the store is full; friction braking becomes dominant not because the motor/inverter has reached a limit but simply because there is no more room on the storage path for power to be pumped. The optimal framework overcomes this through incorporating the braking-converter–related constraints - charger limitations, SOC limits of batteries, supercapacitor voltage maximums and DC link restrictions—into the traction power apportioning process. Effectively, the response of the controller is that it trades off small degradation in today’s energy power split between traction and electricity for bigger gains in recoverable braking power later, which is why the biggest improvements are clustered around urban and aggressive cycles where a lot of braking happens and there are many opportunities to recover energy.

From a field deployment perspective, multi-objective metaheuristics offer an obvious advantage to single-objective tuning and highly hand-crafted rule sets. Instead of constructing a single “best” controller which could potentially overfit any particular drive

International Journal of Engineering Research & Technology (IJERT)
ISSN: 2278-0181
Vol. 14 Issue 12 , December - 2025

cycle, the offline optimization yields a Pareto set of feasible policies covering selective hydro-gen economy, maximum regeneration and minimum component stress within the same hard constraints. This is important for real operation conditions since FCEVs encounter no single driving regime. One reward policy is good for cruising on the highway, but not necessarily for stop and go traffic or in hilly terrain. The Pareto-based approach describes this variability and offers the possibility that a practitioner can choose an operating point according to their application (e.g., fleet vehicle focused on durability, passenger vehicle focused on fuel economy, urban bus focused on regeneration and brake wear) and process in real time using fast lookup and constraint enforcement. This architecture also renders the approach computationally attractive: costly search is performed in the offline phase while online computation consists of lightweight candidate selection, interpolation, and feasibility checks.

The numerical results also elucidate the clear and pronounced contribution of the supercapacitors when it is explicitly designed (not just merely as an additional secondary buffer). In the integrated design, the supercapacitor serves as a major "shock absorber" of the high-power electrical powertrain. During tractive, it stores and returns high frequency power components, which would otherwise force accelerated ramps of the fuel cell or large battery currents. That's because during regenerative braking it captures short duration, high power bursts of regen that can easily exceed battery acceptance limits when under aggressive decel. This dual mode has three tangible advantages, namely 1) it provides stability to fuel-cell operation by minimizing ramping and current ripple, hence enhancing efficiency margins due to the reduced stress on air-path/humidification subsystems; 2) it lowers battery peak currents and cycling severity – which are intimately related to battery heating and aging mechanisms; and 3) it maximizes recuperation of braking energy in actual terms, especially during stop–go driving where regeneration events are frequent yet highly pulsed. These effects are multiplicative: Improved transient buffering enhances fuel-cell efficiency and preserves storage headroom, which also raises regen capture and shifts away from using friction brakes most of the time, for a more efficient & durable system overall.

In practical terms, the unified framework brings design and calibration decisions that are of importance to manufacturers and fleet operators. It also can decrease hydrogen consumption and brake wear (through increase of the regenerative contribution), and driver battery aging (by decreasing RMS current, peak) current. It also provides a principled way to enforce safety and drivability constraints—through explicit constraint handling and smooth brake blending instead of ad hoc limits that may compromise performance in uncharacterized ways. Taken together, the simulations indicate that for the most relevant real-world gains, operations with high frequency of transients and braking—urban drive cycles, delivery duty cycles and aggressive driving—where both integrated optimization and explicit supercap utilization offer the greatest leverage in efficiency, recovery and component life.

IV. CONCLUSIONS

This work proposed an online multi-agent system based regenerative braking optimization in fuel-cell electric vehicles, with energy management and metaheuristic optimizer-generated supervisory setpoints and fast inner loops for DC–DC/inverter regulation and torque tracking. The power management policy not only governed hydrogen consumption, battery-aging proxies (RMS/peak current and SOC excursions), DC-link voltage deviation as well friction-brake use under constraints (fuel-cell ramp/slew limits, source current bounds, and SOC/voltage windows), but allowed coordinated source role separation and uniform transient momentum-serving. Over representative transient-rich drive cycles, DC-link regulation was significantly improved: peak sag/overshoot and recovery time for the DC-link were reduced with general findings of 30–60% lower peak voltage excursions and 20–40% less of the ripple on the DC-link compared to baseline PI-tuned/RB during aggressive torque steps and pulse loading. Battery stress was also less with frequency-separated allocation, resulting in 15–35% lower RMS battery current and 30–55% fewer peak-current events at ports, while keeping SOC inside a more restrictive operating range (less deep-discharge exposure). Co-optimizing regenerative braking added electrical braking power and decreased the reliance on friction-braking with ~8–20% more recovered-energy used (cycle-dependent) without loss of time-evolving charging limits or stability. Parameter drift (converter L/R, DC-link capacitance and motor Rs/L) robustness analyses revealed both a smaller number of constraint violations and performance degradation using LSTM compared to fixed-gain baselines — frequently single-digit up to low–double-digit % RMSE increases in the case of torque, where error magnitudes remained larger with some oscillations/actions required in the worst cases.

These benefits need to be verified in future on-the-HL and vehicle experiments, considering absolute magnitudes (directs: g H_2/km, Wh/km recovered, °C thermal rise), under sensor noise and actuator delays. We suggest including preview of route/traffic, on-line calibration for aging and a reduced surrogate or hybrid learned–metaheuristic solvers to enhance robustness and decrease computation time towards successful deployment embedded in real-time.

REFERENCES

[1] Mustafa İnci, Mehmet Büyük, Mehmet Hakan Demir, Göktürk İlbey, "A review and research on fuel cell electric vehicles: Topologies, power electronic converters, energy management methods, technical challenges, marketing and future aspects," Renewable and Sustainable Energy Reviews, Volume 137, 2021, 110648, ISSN 1364-0321, https://doi.org/10.1016/j.rser.2020.110648.

[2] V. Paladini, T. Donateo, A. de Risi, and D. Laforgia, "Super-capacitors fuel-cell hybrid electric vehicle optimization and control strategy development," *Energy Conversion and Management*, vol. 48, no. 11, pp. 3001–3008, 2007, doi: 10.1016/j.enconman.2007.07.014.

International Journal of Engineering Research & Technology (IJERT)
ISSN: 2278-0181
Vol. 14 Issue 12 , December - 2025

[3] N. Sulaiman *et al*., "Optimization of energy management system for fuel-cell hybrid electric vehicles: Issues and recommendations," *Applied Energy*, vol. 228, pp. 2061–2079, 2018, doi: 10.1016/j.apenergy.2018.07.087.
[4] V. K. R. Kasimalla and A. Velisala, "A review on energy allocation of fuel cell/battery/ultracapacitor for hybrid electric vehicles," *International Journal of Energy Research*, 2018, doi: 10.1002/er.4166.
[5] Guo, Jinquan, Hongwen He, Chunchun Jia, and Shanshan Guo. 2025. "The Energy Management Strategies for Fuel Cell Electric Vehicles: An Overview and Future Directions" World Electric Vehicle Journal 16, no. 9: 542. https://doi.org/10.3390/wevj16090542.
[6] S. O. Showers *et al*., "State-of-the-art review of fuel cell hybrid electric vehicle energy management," *AIMS Energy*, 2022, doi: 10.3934/energy.2022023.
[7] H. Li, A. Ravey, A. N'Diaye, and A. Djerdir, "A novel equivalent consumption minimization strategy for hybrid electric vehicle powered by fuel cell, battery and supercapacitor," *Journal of Power Sources*, 2018, doi: 10.1016/j.jpowsour.2018.05.078.
[8] H. Li *et al*., "Online adaptive equivalent consumption minimization strategy for fuel cell hybrid electric vehicle considering power sources degradation," *Energy Conversion and Management*, 2019, doi: 10.1016/J.ENCONMAN.2019.03.090.
[9] K. Song *et al*., "Pontryagin's minimum principle-based real-time energy management strategy for fuel cell hybrid electric vehicle considering both fuel economy and power source durability," *Energy*, vol. 205, 2020, doi: 10.1016/j.energy.2020.118064.
[10] J. P. Torreglosa, P. García, L. M. Fernández, and F. Jurado, "Predictive Control for the Energy Management of a Fuel-Cell–Battery–Supercapacitor Tramway," *IEEE Trans. Ind. Informatics*, vol. 10, no. 1, pp. 276–285, 2014, doi: 10.1109/TII.2013.2245140.
[11] X. Hu, L. Johannesson, N. Murgovski, and B. Egardt, "Longevity-conscious dimensioning and power management of the hybrid energy storage system in a fuel cell hybrid electric bus," *Applied Energy*, vol. 137, pp. 913–924, 2015, doi: 10.1016/j.apenergy.2014.05.013.
[12] D. Shen, C. -C. Lim and P. Shi, "Fuzzy Model Based Control for Energy Management and Optimization in Fuel Cell Vehicles," in IEEE Transactions on Vehicular Technology, vol. 69, no. 12, pp. 14674-14688, Dec. 2020, doi: 10.1109/TVT.2020.3034454.
[13] X. Cheng *et al*., "Multi-objective adaptive energy management for fuel cell hybrid vehicles considering degradation and energy efficiency," *Applied Thermal Engineering*, 2024, doi: 10.1016/j.applthermaleng.2024.124270.
[14] L. Guo, Z. Li and R. Outbib, "Reinforcement Learning based Energy Management for Fuel Cell Hybrid Electric Vehicles," *IECON 2021 – 47th Annual Conference of the IEEE Industrial Electronics Society*, Toronto, ON, Canada, 2021, pp. 1-6, doi: 10.1109/IECON48115.2021.9589725.
[15] Fayyazi, Mojgan, Paramjotsingh Sardar, Sumit Infent Thomas, Roonak Daghigh, Ali Jamali, Thomas Esch, Hans Kemper, Reza Langari, and Hamid Khayyam. 2023. "Artificial Intelligence/Machine Learning in Energy Management Systems, Control, and Optimization of Hydrogen Fuel Cell Vehicles" *Sustainability* 15, no. 6: 5249. https://doi.org/10.3390/su15065249.
[16] Zeng, Sheng, Hongwen He, and Jingda Wu. 2025. "Proactive Energy Management for Fuel Cell Hybrid Vehicles: An Expert-Guided Slope-Aware Deep Reinforcement Learning Approach" *Energies* 18, no. 22: 6054. https://doi.org/10.3390/en18226054.
[17] J. Zhang *et al*., "A joint strategy of energy management and energy braking recovery for fuel cell vehicles considering ultracapacitor," *Renewable and Integrative Energy Reviews*, 2025, doi: 10.1016/j.rineng.2025.106449.
[18] E. M. Szumska, "Regenerative Braking Systems in Electric Vehicles: A Comprehensive Review of Design, Control Strategies, and Efficiency Challenges," *Energies*, vol. 18, no. 10, p. 2422, 2025, doi: 10.3390/en18102422.
[19] Saiteja P, Ashok B, Wagh AS, Farrag ME. Critical review on optimal regenerative braking control system architecture, calibration parameters and development challenges for EVs. *Int J Energy Res*. 2022; 46(14): 20146-20179. doi:10.1002/er.8306.
[20] Szumska, Emilia M. 2025. "Regenerative Braking Systems in Electric Vehicles: A Comprehensive Review of Design, Control Strategies, and Efficiency Challenges" *Energies* 18, no. 10: 2422. https://doi.org/10.3390/en18102422.
[21] Liu, Hanwu, Yulong Lei, Yao Fu, and Xingzhong Li. 2020. "Multi-Objective Optimization Study of Regenerative Braking Control Strategy for Range-Extended Electric Vehicle" *Applied Sciences* 10, no. 5: 1789. https://doi.org/10.3390/app10051789.
[22] G. Le Solliec, A. Chasse, and M. Geamanu, "Regenerative braking optimization and wheel slip control for a vehicle with in-wheel motors," *IFAC Proc. Vol.*, vol. 46, no. 21, pp. 542–547, 2013, doi: 10.3182/20130904-4-JP-2042.00043.
[23] Y. Yao, Y. Zhao, and M. Yamazaki, "Integrated regenerative braking system and anti-lock braking system for hybrid electric vehicles & battery electric vehicles," *SAE Int. J. Adv. Curr. Pract. Mobility*, 2020, doi: 10.4271/2020-01-0846.
[24] C. A. C. Coello Coello, G. T. Pulido, and M. S. Lechuga, "Handling multiple objectives with particle swarm optimization," *IEEE Trans. Evol. Comput.*, vol. 8, no. 3, pp. 256–279, 2004, doi: 10.1109/TEVC.2004.826067.
[25] K. Deb, A. Pratap, S. Agarwal, and T. Meyarivan, "A fast and elitist multiobjective genetic algorithm: NSGA-II," *IEEE Trans. Evol. Comput.*, 2002, doi: 10.1109/4235.996017.
[26] Tang, Kezong, and Chengjian Meng. 2024. "Particle Swarm Optimization Algorithm Using Velocity Pausing and Adaptive Strategy" *Symmetry* 16, no. 6: 661. https://doi.org/10.3390/sym16060661.
[27] A. M. Reza *et al*., "Investigating the Potential of a New Green Hydrogen Production Method in Indonesia: Thermochemical Water-Splitting," *2025 International Conference on Technology and Policy in Energy and Electric Power (ICT-PEP)*, Yogyakarta, Indonesia, 2025, pp. 97-102, doi: 10.1109/ICT-PEP67281.2025.11232340.
[28] Zhao Liu, Huicui Chen, Tong Zhang, "Review on system mitigation strategies for start-stop degradation of automotive proton exchange membrane fuel cell," Applied Energy, Volume 327, 2022, 120058, ISSN 0306-2619, https://doi.org/10.1016/j.apenergy.2022.120058.